



Heartbeat Resonance: Inducing Non-contact Heartbeat Sensations in the Chest

Waseem Hassan

Department of Computer Science
University of Copenhagen
Copenhagen, Denmark
waha@di.ku.dk

Sonia Elizondo

Universidad Pública de Navarra
Pamplona, Spain
sonia.elizondo@unavarra.es

Liyue Da

The University of Copenhagen
Copenhagen, Denmark
fgp973@alumni.ku.dk

Kasper Hornbæk

Department of Computer Science
University of Copenhagen
Copenhagen, Denmark
kash@di.ku.dk

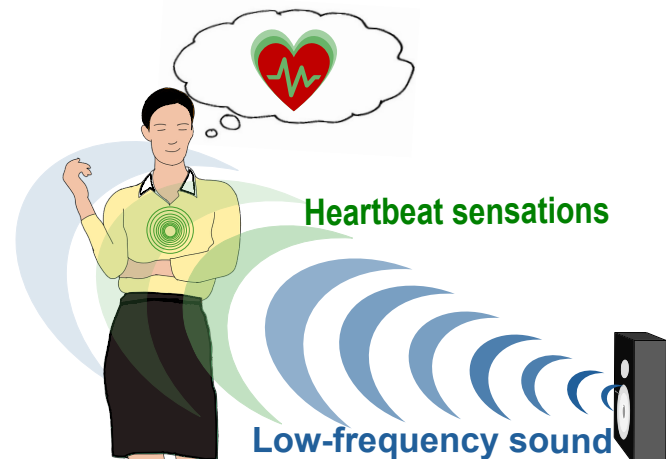


Figure 1: Heartbeat signals are modulated using low-frequency sound waves to create the perception of heartbeat sensations within the user's chest cavity.

Abstract

Perceiving and altering the sensation of internal physiological states, such as heartbeats, is key for biofeedback and interoception. Yet, wearable devices used for this purpose can feel intrusive and typically fail to deliver stimuli aligned with the heart's location in the chest. To address this, we introduce Heartbeat Resonance, which uses low-frequency sound waves to create *non-contact* haptic sensations in the chest cavity, mimicking heartbeats. We conduct two experiments to evaluate the system's effectiveness. The first experiment shows that the system created realistic heartbeat sensations in the chest, with 78.05 Hz being the most effective frequency. In the second experiment, we evaluate the effects of entrainment by simulating faster and slower heart rates. Participants perceived the

intended changes and reported high confidence in their perceptions for +15% and -30% heart rates. This system offers a non-intrusive solution for biofeedback while creating new possibilities for immersive VR environments.

CCS Concepts

- Human-centered computing → Mixed / augmented reality; Haptic devices.

Keywords

Vibrotactile feedback; non-contact haptics; psychophysics; heartbeat modulation

ACM Reference Format:

Waseem Hassan, Liyue Da, Sonia Elizondo, and Kasper Hornbæk. 2025. Heartbeat Resonance: Inducing Non-contact Heartbeat Sensations in the Chest. In *CHI Conference on Human Factors in Computing Systems (CHI '25)*, April 26–May 01, 2025, Yokohama, Japan. ACM, New York, NY, USA, 22 pages. <https://doi.org/10.1145/3706598.3713959>



This work is licensed under a Creative Commons Attribution-NonCommercial 4.0 International License.

CHI '25, Yokohama, Japan

© 2025 Copyright held by the owner/author(s).

ACM ISBN 979-8-4007-1394-1/25/04

<https://doi.org/10.1145/3706598.3713959>

1 Introduction

As our daily lives become more intricate and demanding, the need to understand and engage with our internal physiological states is growing increasingly important [37]. Disruptions to physiological balance can affect cognitive performance [51] and overall health [1, 80]. Within this context, human-computer interaction (HCI) is uniquely positioned to create physiological computing systems to enhance our ability to perceive and regulate internal states [32, 47]. Biofeedback is one such approach, where physiological data is used to help individuals regulate bodily functions that are typically outside conscious awareness [10, 55].

While traditional biofeedback has effectively enhanced awareness and control over physiological states, entrainment offers a complementary alternative. Entrainment uses external stimuli to influence and synchronize with physiological rhythms [8]. Unlike biofeedback, which often requires active user engagement to consciously regulate internal states, entrainment is a more passive process. This approach guides the body's rhythms through external modulation without conscious effort.

A critical area of innovation in this paradigm is developing methods that effectively target interoception—the process of perceiving, interpreting, and integrating signals from within the body [13]. Enhanced interoceptive ability is crucial for emotional regulation [30] and social cognition [6], with abnormalities in this process linked to conditions such as depression [48], anxiety [79], and neurodegenerative diseases [11]. Interoception enables individuals to better understand and respond to their body's signals, which can lead to better informed and healthier behaviors.

Entrainment feedback is often delivered using the same methods as biofeedback. The key difference is that biofeedback senses internal body signals and replays them, whereas entrainment guides the body's signals to align with an external rhythm. Typically it is delivered as visual [3, 93], auditory [59, 69], or haptic feedback mechanisms [21, 61]. Visual feedback often involves graphs or images on screens; auditory feedback might use tones or beeps; and haptic feedback usually comes in the form of vibrations or physical manipulations. Real-time haptic feedback appears to significantly improve interoceptive ability and shift attention towards bodily sensations, compared to visual or auditory feedback [21, 102]. Yet, the haptic feedback is delivered through physical devices that may be cumbersome and restrict movement and comfort. The feedback location, in some cases, might not align with the origin of the biosignals, such as the chest for heartbeat feedback [98, 105]. These factors can degrade the overall user experience and comfort.

To address these limitations, we propose *Heartbeat Resonance*, a system for inducing non-contact haptic sensations of heartbeats using low-frequency sound waves. Low-frequency sounds can create standing waves in an acoustically sealed environment. These standing waves generate pressure fields with specific spatial distributions. The pressure fields, when hitting a person, can induce haptic sensations in different parts of the body [43]. By leveraging this phenomenon, we design a digital heartbeat signal and modulate it with the low frequencies. This enables us to effectively simulate the sensation of a heartbeat in the user's chest cavity without physical contact, offering a novel and potentially more comfortable way to deliver feedback.

In this paper, we discuss the design and implementation of *Heartbeat Resonance* and present its perceptual and physical impact on participants. In Section 4, we explain how we developed the system and designed the digital heartbeat signals. We validate the system's ability to produce realistic heartbeat sensations in a user study, detailed in Section 5. In this study, participants were exposed to digital heartbeat signals modulated at various low frequencies. Their responses allowed us to identify the optimal frequency and signal characteristics that created the most realistic heartbeat sensations. In a second user study, participants were exposed to digital signals designed to simulate increased and decreased heart rates to encourage entrainment. We assessed participants' ability to perceive the heart rate changes, their confidence in these perceptions, and the system's influence on their actual heart rates (see Section 6). This experiment explored whether participants' heart rates could follow the delivered signals of simulated increases or decreases. Our findings demonstrate that the system produced realistic sensations in the chest cavity and showed evidence of entrainment, indicating potential applications in everyday life and diverse settings (see Section 7).

2 Related Work

We begin by exploring the various forms of biofeedback and entrainment—visual, auditory, and haptic—and the role of biofeedback on interoceptive ability. We also discuss the different parameters used to modulate heart rate feedback. Finally, we highlight the major underlying theoretical foundations that explain how heart rate biofeedback works.

2.1 Biofeedback And Entrainment

Biofeedback is extensively addressed in the form of visual, auditory, and tactile cues, or a combination of them [68]. Designing these types of feedback can be challenging as individuals might interpret them differently depending on their cultural or personal beliefs [70, 71]. One relevant way of sharing biofeedback is through visualization [22, 76, 77]. It effectively transforms invisible data into a visual form that users can easily understand and use to obtain information [36]. For instance, Miner et al. [73] altered participants' breathing rate through visuals in Virtual Reality, while Leslie et al. [59] did so by using auditory feedback. Another form is tactile biofeedback, which has been used for improving body posture and balance [95, 96].

Among biofeedback solutions, heartbeat biofeedback stands out as a relevant source of physiological information and a means to enhance bodily awareness [88]. Fang et al. [33] demonstrated how visual heartbeat signals shared among players in a face-to-face game could influence decision-making. Similar experiences have been reported when using mobile applications and wearable devices to share visual heartbeat representations [19, 44, 64, 65]. Other modalities include auditory cues [46] and haptic feedback, such as vibrations delivered to the chest or fingers [91, 98].

Building on these approaches, entrainment offers an additional way to actively influence physiological rhythms through external stimuli [8]. Entrainment is the natural process where biological rhythms, like heartbeats or breathing, align with repeating patterns such as sounds [85, 100], lights [2, 89], or tactile pulses [87]. This

alignment occurs because the body responds to rhythmic inputs, allowing external stimuli to guide internal processes. For instance, vibrations [87] or visual [57] cues can encourage the heart to beat in sync with the stimulus, promoting relaxation [39, 105]. Other signals, such as breathing [75, 85] or brainwaves [7, 104], can also be influenced through entrainment. While biofeedback and entrainment systems share similar mechanisms, biofeedback emphasizes awareness and voluntary control, while entrainment focuses on passive synchronization through carefully designed stimuli.

Heartbeat biofeedback and entrainment have been shown to improve empathy between users [44, 66] and induce calming effects [46, 105]. It is particularly beneficial for people with anxiety and stress [40, 101]. Following this path, we present *Heartbeat Resonance*, a non-contact haptic feedback system that delivers heartbeat sensations inside the chest cavity. This solution addresses the possibility of feeling a heartbeat without requiring the user to equip any devices.

2.2 Interoception

Interoception [13, 38] refers to the awareness and perception of internal bodily sensations, such as a racing heart after a sudden fright or a growling stomach when hungry. It plays an important role in emotion regulation, decision-making, and overall well-being [45, 50]. Awareness of these bodily signals can significantly impact how emotions are processed and regulated, and it is closely linked to various psychological conditions, such as trauma [78], anxiety [23, 42, 83], self-regulation [31], and alexithymia [103].

Research has shown that biofeedback interventions, including visual, auditory, and haptic feedback, can enhance interoceptive abilities, helping individuals become more in tune with their internal signals [9, 35]. For example, Ashton et al. [5] demonstrated that visual feedback can improve heartbeat perception accuracy, while Schandry et al. [84] showed that auditory feedback can help slow heart rate. Dobrushina et al. [21] employed both haptic and visual systems to enhance cardiac interoception, with haptic biofeedback proving more effective than visual feedback. Although not explicitly explored, a possible effect of *Heartbeat Resonance* could be an increased awareness of internal bodily states, possibly contributing to positive effects such as improved emotional regulation and well-being.

2.3 Parameters for Heart Rate Modulation

The delivery of heart rate biofeedback has been widely studied in the fields of psychology, health, and HCI. Different approaches have been employed to modulate the parameters for delivering heartbeat sensations, focusing on aspects such as sensory modality, frequency/Beats Per Minute (BPM) selection, and area of application.

Different sensory modalities have been used to deliver heart rate feedback, including visual, auditory, and haptic approaches. Visual feedback [3, 22, 76, 77, 93], such as flashing lights or graphical representations, is effective for detailed monitoring and when visual attention is available, though it may be limiting in more immersive scenarios. Auditory feedback [59, 69, 95, 96], involving rhythmic sounds or tones, helps evoke emotional responses, enhancing participants' awareness of their physiological state and aiding relaxation or arousal. Haptic feedback [14, 21, 92, 98, 105],

particularly vibrotactile, allows users to physically feel their heart rate, fostering a sense of bodily presence. The specific application and intended experience largely dictate the choice of modality.

The BPM of heart rate is a well-explored parameter for biofeedback and entrainment. BPM can be the same as the real heart rate of the user, higher or lower. The same BPM heart rate feedback is typically used for biofeedback, while entrainment uses external rhythms (with higher, lower, or matching BPM) to guide synchronization [56]. We discussed the utility of biofeedback in Section 2.1. Studies have shown that a higher BPM can lead to excitement, arousal, fear, or nervousness [16, 54, 97], while a lower BPM can induce relaxation or reduce anxiety [15, 20, 82]. There are two common strategies for selecting BPM: using percentages to adjust the heart rate (e.g., increasing by 15%) [16, 20, 25] and using fixed values for higher or lower BPM [14, 15, 92]. Both strategies have their advantages; percentage adjustments allow for a more personalized response based on the user's baseline, while fixed values can simplify the setup and ensure consistency across participants.

Another important consideration is the area of delivery on the body. Wrist-worn devices [14, 15, 97] have been the most common method of delivering heartbeat feedback. However, other body parts, such as the chest [21, 91, 92], neck [92], ankles [92], and hand [98, 105], have also been explored. The chest might be suggested as the most effective area, as it aligns with the natural origin of the heartbeat, potentially enhancing the perceived realism [21]. In contrast, the wrists or hands are reported to be less effective [92]. However, if the aim is to deliver feedback discreetly, the ankles can be a suitable option, due to lower awareness of sensations [92].

2.4 Theoretical Foundations of Heart Rate Biofeedback

Heart rate biofeedback (HRB) is a method that allows individuals to gain voluntary control over their autonomic functions, particularly heart rate, by providing real-time feedback. This method has been shown to improve physiological regulation and emotional well-being [55]. Based on the available literature on HRB, we discuss five of the more prominent theories that explain HRB: Operant Conditioning [28], the Psychophysiological Principle [86], the Baroreceptor Reflex [24], the Resonance Frequency Phenomenon [57], and Vagal Afferent Pathways [18].

One of the earliest theories underlying HRB is *Operant Conditioning* [27, 28, 72]. Developed in the 1960s, this theory suggests that individuals can learn to control their physiological responses through reinforcement. In HRB, real-time feedback on heart rate serves as a form of reinforcement, encouraging behaviors that lead to desired outcomes, such as lowered heart rate or increased heart rate variability [29].

Building on the foundation of operant conditioning, the *Psychophysiological Principle* [86] was introduced in the 1970s. This theory highlights the direct relationship between physiological and psychological states. By making individuals aware of their physiological signals, such as heart rate, HRB enables them to regulate their mental and emotional states more effectively. This connection between body and mind has been crucial in understanding how biofeedback can improve both physical health and psychological well-being [26].

In the 1990s, the **Baroreceptor Reflex** [24] was recognized as a key theory in HRB. This reflex involves the body's natural ability to regulate heart rate and blood pressure through feedback loops mediated by baroreceptors. In HRB, the baroreceptor reflex is engaged by simulating changes in heart rate, which can then influence blood pressure and trigger further adjustments in heart rate, creating a dynamic feedback loop that supports cardiovascular stability [58, 60, 94].

The **Resonance Frequency Feedback** [57] theory, which gained prominence in the 2000s, involves synchronizing breathing and heart rate oscillations at a specific resonance frequency, typically around 0.1 Hz. This synchronization maximizes heart rate variability (HRV), which is associated with better cardiovascular health and greater resilience to stress [53]. It also leads to better gas exchange during respiration, enhanced oxygen delivery to tissues, and overall improved autonomic balance [94].

The most recent development in HRB theory is the **Vagal Afferent Pathways** [18], which became prominent in the 2010s. These pathways connect the heart and brain via the vagus nerve. HRB stimulates these pathways by enhancing vagal tone (the level of activity of the vagus nerve). Increased vagal tone is associated with greater parasympathetic activity, promoting relaxation and reducing stress [81]. This process positively influences brain areas involved in emotional regulation, which are crucial for processing emotions and bodily sensations [49, 52].

3 Creating Non-Contact Tactile Sensations

Heartbeat Resonance aims to induce non-contact heartbeat sensations in the chest, as outlined in the introduction. To achieve this, we took inspiration from a recent study where non-contact haptic sensations were successfully delivered to the whole body using low-frequency sounds [43]. This approach enables our goal of providing non-contact heartbeat sensations. We recreated this system for our study, allowing us to deliver tactile sensations without requiring the user to wear or touch any device. It should be noted that the system proposed by Hassan et al. [43] was neither developed nor evaluated to deliver heartbeat sensations, but was instead designed to provide monotonic haptic feedback. We first explain how the non-contact system works, and in Section 4 we discuss how we adapted it to deliver non-contact heartbeat sensations in the chest.

3.1 Materials

The experiments were conducted in a specially constructed room designed to optimize the reflectance and control of low-frequency sounds, shown in Fig. 2. The room was built from medium-density fiberboard (MDF) and had dimensions of 1.7m × 2.18m × 2.12m. To deliver the low-frequency sound signals, we used an SB 4000 subwoofer by SVS¹, which is capable of producing up to 300 Hz frequencies with peak amplitude of 126.8 dB. The subwoofer was positioned centrally along the y-axis. The signals were relayed to the subwoofer through a Scarlett 6i6 pre-amplifier².

¹SVS SB 4000 Subwoofer

²The Scarlett 6i6 2nd Generation is discontinued. See Scarlett 4i4 4th Generation.

3.2 Theoretical Basis

The system operates by emitting low-frequency sound waves from a subwoofer, which then reflect off the walls of an acoustically sealed room. These sound waves interact to form standing waves, creating zones of high (antinodes) and low (nodes) acoustic pressure. This spatial distribution of pressure, known as room modes, depends on the room's dimensions and the frequency of the sound waves. When the standing waves come into contact with a person, they experience tactile sensations corresponding to the pressure of the standing wave at the point of contact [43, 74]. This pressure distribution of the standing waves is predictable, which enables the delivery of the controlled tactile sensations to the whole body, or localized to specific regions.

3.3 Simulation of Standing Waves

Every room has specific modes (frequencies) at which strong standing waves are formed. The modal response (a set of modes) of the current room was calculated using $f_{pqrs} = \frac{c}{2} \sqrt{\left(\frac{p}{L_x}\right)^2 + \left(\frac{q}{L_y}\right)^2 + \left(\frac{r}{L_z}\right)^2}$, where f_{pqrs} is the frequency of the mode with indices p , q , and r ; c is the speed of sound; and L_x , L_y , and L_z are the dimensions of the room. This equation identified 14 modal frequencies below 200 Hz – 78.05, 80.26, 100.09, 111.95, 126.92, 128.29, 150.17, 156.1, 160.51, 175.53, 178.49, 185.44, 189.17, and 200.18 Hz. The 200 Hz limit was chosen because simulating standing waves at higher frequencies becomes increasingly challenging due to the added complexities and interactions within the acoustic environment.

The pressure distribution of each of these frequencies was simulated using the Helmholtz equation for wave propagation [34]. The Helmholtz equation was solved using Finite Element Analysis (FEA) as it allows for precise modeling of the acoustic wave behavior. This provided us with the pressure distributions for each of the frequencies throughout the room, giving us a detailed understanding of where the strongest haptic sensations would occur.

We used a specific room in our current setup, as described in Section 3.1. However, the system can be implemented in rooms with different sizes and reflectivity of the walls. This would require the above process to be repeated for the new room. The dimensions of the new room would determine the room's modal response, followed by FEA simulations of the standing waves in the room. We provide code in Appendix A to model and simulate the spatial distribution of pressure in a new environment. After calculating the areas of high pressure from the spatial distribution, the setup in Section 4 can be followed to set up *Heartbeat Resonance*. Appendix A.1 includes code for modeling walls with varying reflectivity. Appendix A.2 provides code for incorporating objects into the simulation, as these can affect the propagation of standing waves.

3.4 Delivering Tactile Sensations

This system can produce non-contact tactile sensations, however, we are especially interested in the emergent properties highlighted in the previous study [43], such as the ability of low-frequency sounds to generate sensations perceived *inside the body*. This emergent property aligns with our goal of simulating realistic heartbeat sensations and achieving entrainment. In the following section, we explain how we adapted the system for our purpose.

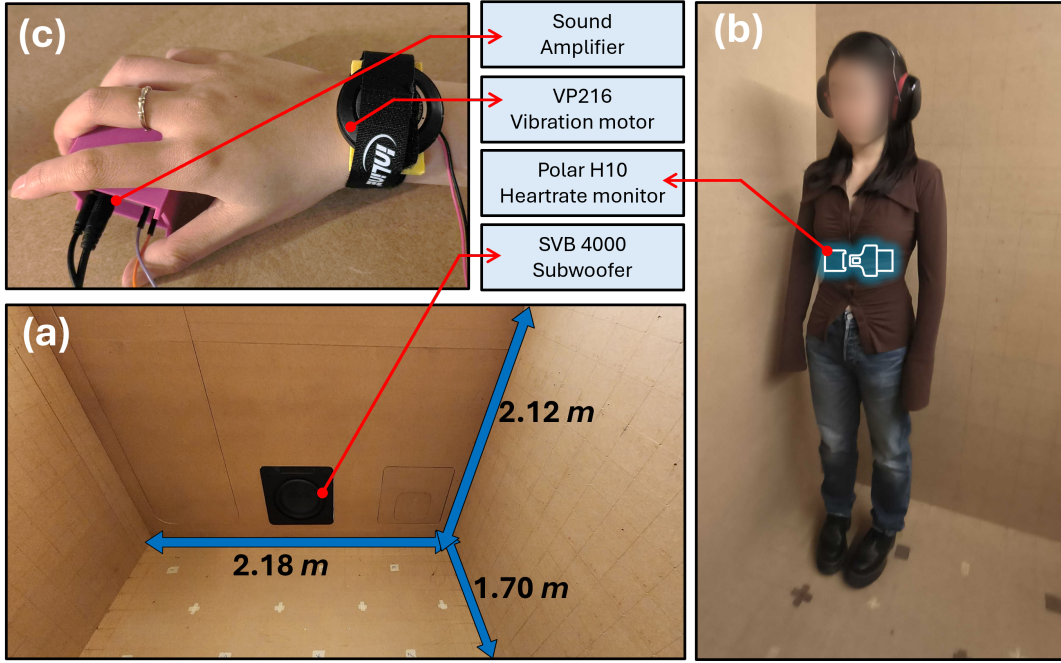


Figure 2: (a) The room where the experiment took place, showing the dimensions and the position of the subwoofer used to deliver low-frequency vibrations for Heartbeat Resonance. (b) The *Heartbeat Resonance* condition where the participant experienced non-contact sensations in the chest area. (c) The condition where the participant experiences vibrotactile feedback on the wrist. Participants wore a Polar H10 heart rate monitor in both conditions for Experiment 2.

4 Non-contact Heartbeat Sensations

In this section, we discuss how we utilized low-frequency sounds to create non-contact heartbeat sensations. While Hassan et al. [43] employed constant sine waves to deliver monotonous sensations, the dynamic nature of a heartbeat is different. Heartbeat signals are characterized by distinct pulses and variability, making them challenging to replicate with low-frequency sound waves. The key challenge was to ensure that adapting the signals to simulate heartbeats would preserve the emergent properties while effectively generating the desired heartbeat sensations in the chest area. In the following subsections, we describe how we approached this adaptation.

4.1 Digital Signal Creation

The digital heartbeat signal was created by replicating the key components of a real heartbeat signal. A heartbeat signal is composed of three main elements: the “lub” (S1), which is the primary pulse; the “dub” (S2), a quieter secondary pulse; and the “tail”, a faint sound that follows the dub.

We generated each component using a sine wave at 150 Hz. This frequency was empirically selected after experimentation. To make the components sound smooth and natural, we applied an envelope to each one. This envelope gradually increased and decreased the volume, resulting in pulses that rise and fall gently, preventing abrupt transitions.

After generating the “lub”, “dub”, and “tail”, we arranged them into a single heartbeat pattern. The timing between each component was modeled on a reference heart rate of 60 beats per minute (BPM). The entire “lub-dub-tail” sequence was repeated to match the desired duration, with periods of silence between beats to simulate the natural pauses in a real heartbeat signal. This generated a continuous signal that could be played for any arbitrary duration. To achieve different BPMs, we dynamically adjusted the timing to reflect the natural rhythm of a heartbeat, ensuring appropriate gaps between the “lub”, “dub”, and “tail”. Using this process, we created two distinct heartbeat signals:

Basic Heartbeat Signal (Digital 1): The basic signal aimed to replicate the fundamental S1 (lub) and S2 (dub) sounds of a heartbeat, as shown in Fig. 3a. This simple design focused on ensuring that the key elements of a heartbeat were clearly identifiable while staying as close as possible to the conditions highlighted by Hassan et al. [43].

Enhanced Heartbeat Signal (Digital 2): The enhanced signal incorporated the S1 and S2 sounds, along with the tail, as shown in Fig. 3b. This additional component was included to make the heartbeat simulation feel more realistic, offering a more lifelike heartbeat sensation.

4.2 Signal Modulation

Once the heartbeat signal was established, we modulated it with low-frequencies at 78, 100, 150, and 200 Hz. The frequencies of 78

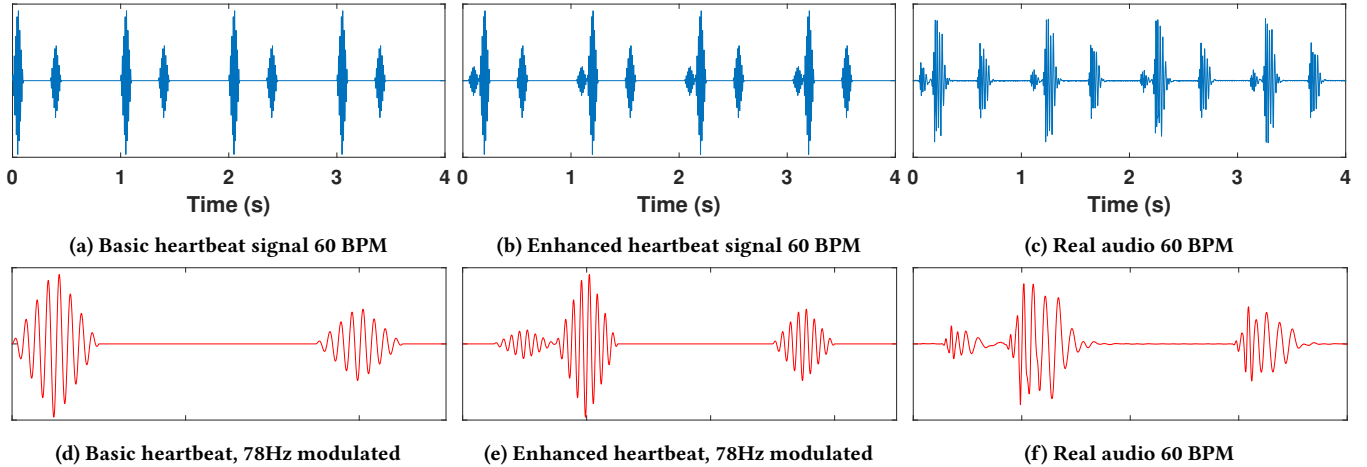


Figure 3: The digital and real heartbeat signals used in Experiment 1. Subfigures (a)–(c) show the three signals at 60 beats per minute (BPM). Subfigures (d)–(f) show close-up views of the signals, (digitally) modulated at 78 Hz, to visualize the modulation frequency.

and 100 Hz were selected based on previous work by Hassan et al. [43], which identified these low frequencies as particularly effective in producing emergent properties, such as the perception of internal sensations. To explore the effects of different frequency ranges, we added two more frequencies: 150 Hz from the midrange and 200 Hz from the high range to observe how these variations impacted the perceived sensations. The basic and enhanced heartbeat signals modulated at 78 Hz are shown in Figs. 3d and 3e, respectively.

4.3 Heartbeat Sensation Delivery

Once the signals were modulated with the selected frequencies, we used the pressure distributions obtained from the FEA simulations in Section 3.3 to predict where in the room the sensations would have the highest pressure.

We calculated the locations of high pressure based on the height of each participant. Participants were instructed to stand in precise positions dictated by the FEA simulations. For each of the selected frequencies—78, 100, 150, and 200 Hz—we identified the locations in the room with the highest pressure at chest level. These locations varied across participants due to differences in standing wave patterns for each frequency and individual participant heights.

5 Experiment 1: Inducing Heartbeat Sensations

In this experiment, we aimed to evaluate the effectiveness of *Heartbeat Resonance* in inducing perceivable heartbeat sensations. We assessed the impact of two digital heartbeat signals alongside a real heartbeat sound. The real heartbeat sound was used as a baseline comparison, consistent with the literature for haptic biofeedback [21]. The findings from this experiment would guide the selection of the most effective signal for subsequent experiments.

5.1 Participants

A total of 14 participants (self-reported gender, eight female and six male) were recruited for the experiment. They reported no

disabilities that would affect their participation, and their ages ranged from 24 to 29 years ($M = 25.71$ years old, $SD = 1.48$). Their height ranged from 158cm to 191cm ($M = 171.91$ cm, $SD = 9.39$ cm). All participants were screened to ensure they had no known cardiovascular or auditory impairments. Informed consent was obtained from each participant. Participants were made aware of their right to withdraw from the study at any point. Participants were compensated €27 (\$30) for their participation. The experiment was approved by the Institutional Review Board.

5.2 Experiment Design

This experiment had two independent variables: heartbeat signal type and modulation frequency of the signal. The dependent variables were the perceived realism of the heartbeat sensations, perceived intensity, the on-body location of the sensations, and the sensation type. We used a within-subjects design for the experiment, where each participant experienced all combinations of the heartbeat signal types and modulation frequencies. The heartbeat signals were played at a steady rate of 70 bpm, reflecting a typical resting heart rate. The details of the variables are in the following subsection.

5.2.1 Independent Variables.

(1). Heartbeat Signal Type had three levels: Basic heartbeat signal (Fig. 3a), enhanced heartbeat signal (Fig. 3b), and real heartbeat sound signal (Fig. 3c).

(2). Modulation Frequency had four levels: 78.05, 100.09, 156.1, and 200.18 Hz

5.2.2 Dependent Variables.

(1) *Perceived Realism*: Participants rated the realism of the heartbeat sensations on a semantic differential scale from 1 (not realistic) to 5 (very realistic). This variable assessed how authentic the participants perceived the induced heartbeat sensations to be.

(2) *Perceived Intensity*: Participants rated the intensity of the heartbeat sensation on a semantic differential scale from 1 (not perceivable) to 5 (very strong). This variable measured the strength of the perceived sensation.

(3) *On Body Location*: Participants indicated the location of the sensation on a body silhouette, specifying where on their body they felt the sensation. The torso was divided into 16 segments, with the entire silhouette containing 28 segments, as shown in Fig. 6b. The torso had more segments since it was expected to receive a high majority of the sensations and we wanted to differentiate their impact.

(4) *Sensation Type*: Participants were asked (in the form of a questionnaire) whether the sensation was felt inside the body, on the surface, both inside and surface, or neither inside nor surface.

Each participant experienced 18 conditions (2 digital signals \times 4 frequencies, plus one real heartbeat signal, each repeated twice). The presentation order of the 9 unique conditions was counterbalanced using Latin squares, while sequences across participants were randomized to control for order effects.

The hypotheses for the experiment were as follows:

- **Hypothesis 1**: There is a significant difference between digital signals (Basic, Enhanced) and the real signal in terms of the dependent variables.
- **Hypothesis 2 (Modulation Frequency Effect)**: The modulation frequency of the digital signals has a significant effect on the dependent variables when compared to the real heartbeat signal.
- **Hypothesis 3 (Signal Type Effect)**: The type of heartbeat signal (Basic or Enhanced) has a significant effect on the dependent variables when compared to the real heartbeat signal.

5.3 Procedure

The experimental conditions were explained to the participants before the experiment. After understanding the procedure, they signed a consent form and filled out the demographics form.

Participants stood in a quiet, controlled environment where the digital and real heartbeat signals were delivered to their chest area. The procedure began with an initial practice period where participants experienced all the signals before the experiment started. Each signal was played for 7 seconds across four different frequency settings. After each condition, participants completed a questionnaire to rate the realism and intensity of the heartbeat sensations and to indicate where they felt the sensations on the body silhouette, as well as the type of sensation experienced. Each trial lasted approximately 1 minute, including time for rating and recording responses. The total session time was approximately 25 minutes per participant.

5.4 Data Analysis and Results

The analysis compared each signal's perceived realism and intensity with the real signal (H_1). It was anticipated that the enhanced heartbeat signal (H_3) and 78.05 Hz modulation (H_2) would be rated highest in realism, as it faithfully mimics a real heartbeat and is

modulated with the frequency that would induce sensations in the chest area. The real heartbeat signal was used as a baseline to assess the impact of the digital signals. The digital signals were expected to perform better than the real heartbeat since they were optimized to deliver sensations inside the chest cavity (H_1).

Perceived Realism: The mean realism scores in Fig. 4a (and Appendix B.1) indicate that both the digital heartbeat signals modulated at 78.05 Hz were rated highest in realism. This suggests that the modulation technique used at this frequency effectively mimics the natural sensation of a heartbeat, making it feel more realistic than the actual physiological sound. In contrast, the realism scores tended to decrease as the modulation frequency increased. This is in line with the literature [43], which reported that the lower frequencies are perceived inside the body, resulting in a more realistic heartbeat sensation.

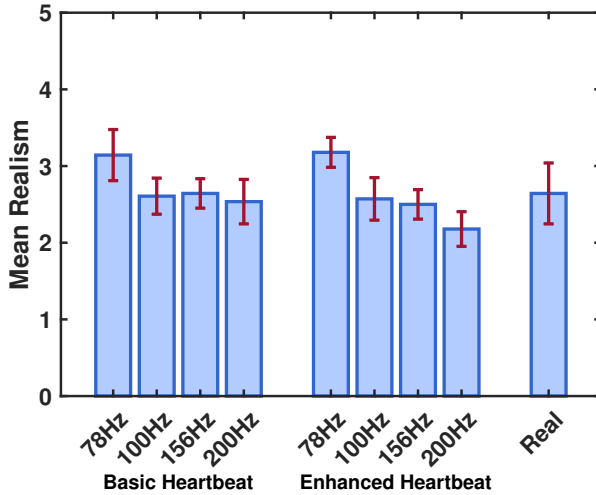
A Friedman test revealed no significant differences when comparing each of the eight digital conditions to the Real signal (H_1). We combined the Basic and Enhanced Heartbeat signals, treating them as instances of a broader category of digital signals. This allowed us to assess whether modulation frequency had any effect on perceived realism (H_2) compared to the real signal. Results showed a significant effect of modulation frequency on realism ratings ($\chi^2(3) = 8.22, p < 0.05$), supporting H_2 . Pairwise comparisons of frequencies using Wilcoxon signed-rank tests revealed that the 78 Hz modulation frequency was significantly different from the Real signal ($z = 2.16, p < 0.05$), as shown in Fig. 5a (and Appendix B.2). This suggests that the specific modulation frequency of 78 Hz contributes to perceived differences.

Additionally, we combined the frequency levels to determine if signal type (Basic vs. Enhanced) had a significant effect across all conditions (H_3). A Friedman test revealed no significant effect of signal type ($\chi^2(1) = 1.06, p > 0.05$).

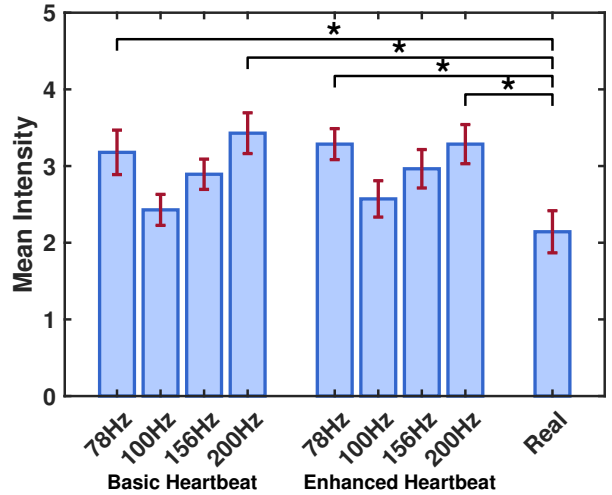
Perceived Intensity: The intensity of the perceived heartbeat sensations was highest at the 200 Hz modulation frequency for both digital signals followed closely by the 78 Hz modulation frequency (200 and 78 Hz are equal for the Enhanced heartbeat signal), as shown in Fig. 4b (and Appendix B.1). The higher frequencies inherently carry more energy, which manifested in higher intensity in our results. Interestingly, realism and intensity have an inverse relationship; while lower frequencies were perceived as more realistic, higher frequencies resulted in more intense sensations (except for 78 Hz). The real heartbeat sound, while moderately intense, did not achieve the same level of perceived intensity as the 78.05 or 200 Hz modulated digital signals.

Pairwise comparisons using Wilcoxon signed-rank tests were conducted to assess differences between the real signal and each experimental condition (H_1). The test showed statistically significant differences between the real signal and both digital signals modulated at 78.05 Hz and 200 Hz ($p < 0.05$), shown in Fig. 4b.

In addition, we assessed the overall effect of modulation frequency (H_2) and signal type (H_3) on intensity ratings, similar to perceived realism. A Friedman test revealed a significant effect of modulation frequency on intensity ratings ($\chi^2(3) = 13.66, p < 0.01$), supporting H_2 . Post-hoc Wilcoxon signed-rank tests showed significant differences between the Real signal and modulation frequencies at 78 Hz ($p < 0.01$), 156 Hz ($p < 0.01$), and 200

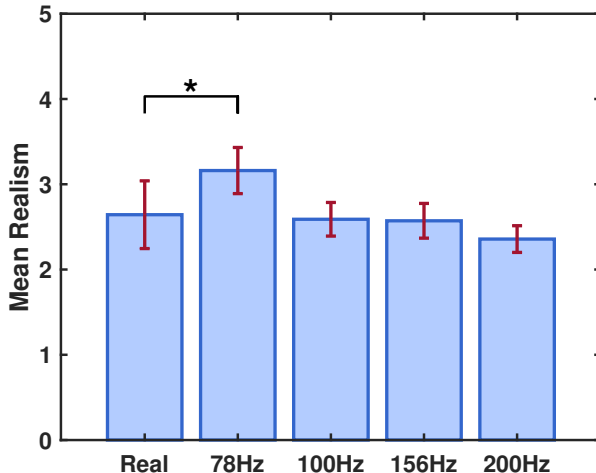


(a) The figure shows the mean realism scores for the two digital signals under different modulation frequencies, and the real signal. Realism was highest for 78 Hz modulation frequency for both digital signals. Full data are in Appendix B.1.

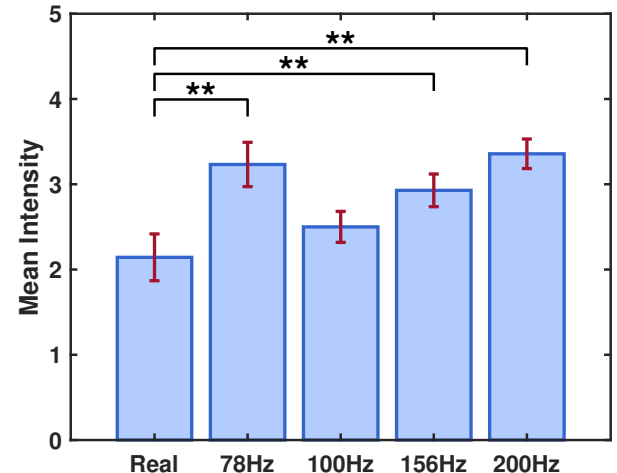


(b) The figure shows the mean intensity ratings for the two digital signals under different modulation frequencies and the real signal. Intensity was highest at 200 Hz modulation frequency for both digital signals. Full data are in Appendix B.1.

Figure 4: The mean realism and intensity scores reported by participants in experiment 1. Error bars show the standard deviation. The asterisk (*) shows $p < 0.05$.



(a) The figure shows mean realism scores for different modulation frequencies. The 78 Hz modulation frequency shows a significant difference from the real signal. Values are provided in Appendix B.2.



(b) The figure shows mean intensity scores for different modulation frequencies. The 78, 156, and 200 Hz modulation frequencies showed significant differences from the real signal. Values are provided in Appendix B.2.

Figure 5: The mean realism and intensity scores showing the effect of modulation frequency. Error bars show the standard deviation. The single asterisk (*) shows $p < 0.05$, and the double asterisk () shows $p < 0.01$.**

Hz ($p < 0.01$), as shown in Fig. 5b (and Appendix B.2). However, there was no significant effect of signal type ($p > 0.05$), failing to accept H₃.

The results indicate that modulation frequency significantly affects both the perceived realism and intensity of the heartbeat sensations. These findings suggest that lower frequencies (such as

78.05 Hz) are more suitable for applications where a realistic heartbeat sensation is desired, such as in biofeedback and entrainment systems. On the other hand, higher frequencies (such as 200 Hz) are better suited for applications that require more intense feedback, like immersive virtual reality systems.

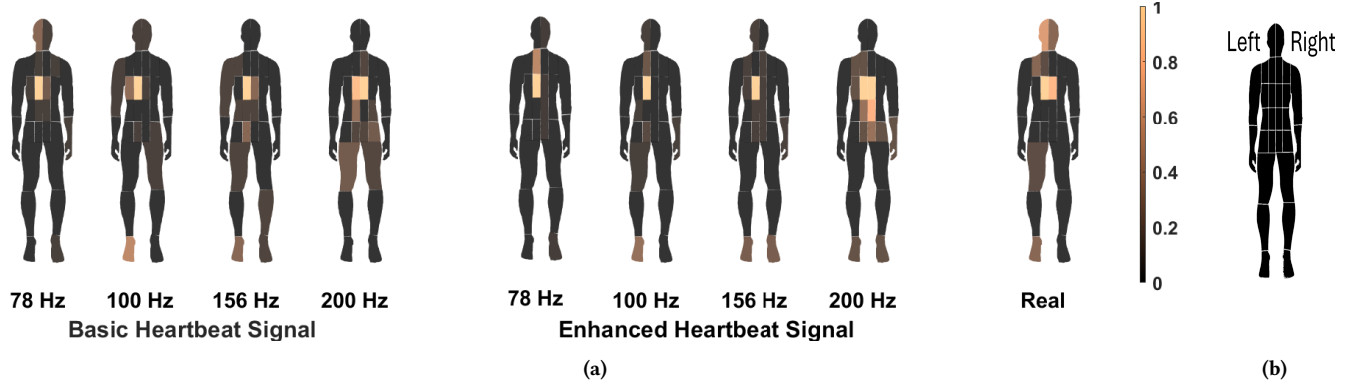


Figure 6: (a) This figure presents a series of silhouette heat maps that visualize the frequency and location of sensations reported by participants across different experimental conditions. Each silhouette represents a different condition: the two digital signals modulated with four different frequencies and a real signal. The color bar on the right provides a scale from 0 (no sensation) to 1 (maximum sensation frequency). Each silhouette is normalized independently to furnish a fair comparison. (b) The rightmost silhouette shows the division of body parts based on which participants selected appropriate body locations of sensations.

On Body Location: The heatmaps in Fig. 6a reveal that sensations are most frequently and intensely felt in the central torso, particularly the chest area, across nearly all the modulated conditions. This consistent pattern suggests that the system effectively targets the chest, which is crucial for simulating heartbeat sensations. However, there is variation in how different conditions affect other body parts. For example, while the chest remains the primary site of sensation, the digital signals at 200 Hz and the real condition produced a more varied sensation pattern, with participants reporting sensations in the head, chest, and lower legs. This variation in sensation distribution indicates that different frequencies influence how and where sensations are felt on the body. Figure 6 suggests that lower frequencies tend to induce more localized sensations, especially in the chest, while higher frequencies may lead to more widespread sensations.

Sensation Type: The heatmaps in Fig. 7 reveal that sensations were most frequently reported as felt inside the body, particularly for conditions using the 78 Hz modulation frequency, with a significant number also reporting feeling sensations both inside and on the surface. Conversely, very few participants reported feeling the sensation only on the surface or not at all. In contrast, the real heartbeat signal was more often perceived on the surface rather than inside.

Based on the findings from Experiment 1 (Inducing Heartbeat Sensations), we selected the 78.05 Hz modulation frequency and the enhanced heartbeat signal for the next experiment, as it produced the most realistic and internally perceived sensations.

6 Experiment 2: Perceived Heart Rate Entrainment

In this experiment, we assessed the participants' ability to perceive external heartbeat signals through perceived entrainment. Perceived entrainment in this context refers to participants' *subjective* experience of their heartbeats synchronizing with the delivered heartbeat sensations (distinct from physiological synchronization,

which is referred to as entrainment). This distinction aligns with research on judged coordination, which shows that people's subjective impressions of being in sync (or entrainment) can differ from actual, measurable coordination [12]. We explored two aspects of participants' responses: their perception of heart rate changes and their confidence in those perceptions.

6.1 Participants

A total of 20 participants (self-reported gender, 10 female and 10 male) were recruited for the experiment. They reported no impairments that would affect their participation. Their ages ranged from 20 to 28 years ($M = 24.56$ years old, $SD = 2.09$). Their height ranged from 160 cm to 187 cm ($M = 171.9$ cm, $SD = 7.27$ cm). The sample size for the user study was estimated using power analysis. The standard deviation and expected significant difference were identified as 2.67 and 4 bmp [41], whereas the power and significance level were set at 0.9 and 0.05, respectively. All participants provided informed consent. Participants were informed of their right to withdraw from the study at any time. They were compensated €40 (\$45) for their participation. The experiment was approved by the Institutional Review Board.

6.2 Experiment Design

The stimuli used in this experiment were based on the enhanced heartbeat signal from Experiment 1, modulated at 78.05 Hz. The signal was varied to simulate different heart rates (BPM). Rather than applying a fixed BPM across all participants, we adjusted the heart rate relative to each participant's baseline. The BPM started at the baseline and linearly increased or decreased to a fixed percentage. This approach, supported by existing literature [20, 25], provides a more tailored and adaptable experience.

6.2.1 Independent Variables. This study had two independent variables: the delivery mechanism and BPM variation.

1) Delivery Mechanism. This variable had two levels:

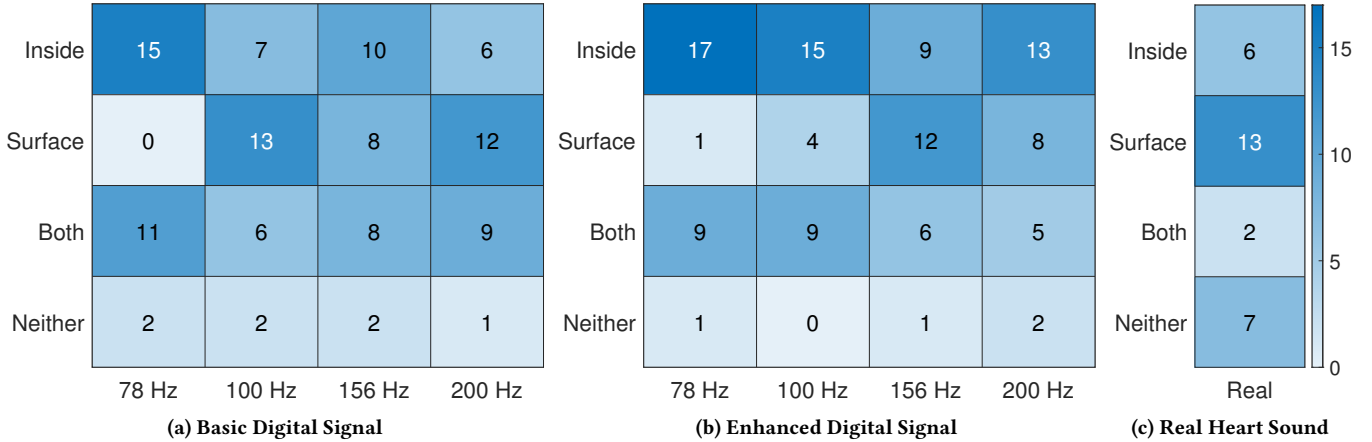


Figure 7: The figure visualizes the frequency of where participants perceived sensations; the options were ‘inside the body’, ‘on the surface’, ‘both inside and on the surface’, and ‘neither inside nor on the surface’. The darker shades indicate higher frequencies of responses.

- *Heartbeat Resonance*: The digital heartbeat signals were delivered via low-frequency sound waves targeting the chest cavity.
- *Vibrotactile Feedback*: In this condition, the heartbeat sensations were delivered through a vibrotactile motor (VP216, Acouve Lab) attached to the participant’s right wrist, simulating a heartbeat through direct vibrations. This allowed us to compare the effect of non-contact haptic feedback with the typically used vibrotactile feedback [102].

2) *BPM Variation*: This variable had two levels, which in turn had two levels for each:

- *Heart Rate Increase*: We used two levels of increased heart rates from baseline: +15% and +30% [20, 25]. These levels were chosen to simulate moderate increases in heart rate to simulate excitement [54].
- *Heart Rate Decrease*: We used two levels of decreased heart rates from baseline: -15% and -30% [20, 25]. These levels were chosen to simulate relaxation or biofeedback interventions [41, 82].

6.2.2 Dependent Variables. This study had two dependent variables: perceived heart rate change and confidence in perception.

1) *Perceived Heart Rate Change*: “Did you feel that your heart rate increased, decreased, or stayed the same during the trial?” This variable assessed their ability to detect the perceived changes in their heart rate in response to the entrainment signal.

2) *Confidence in Perception*: “How confident are you in your assessment of the heart rate change?” (Rated on a scale from 1 = not confident to 5 = very confident). This variable measured how confident the participants were about the assessment of the perceived changes in their heart rate.

The experiment employed a within-subjects design. There were a total of 8 conditions per participant, that is 2 delivery mechanisms and 4 bpm variations (2×4). The presentation order of the

8 conditions was counterbalanced using Latin squares, while sequences across participants were randomized to control for order effects. A Polar H10 heart rate belt was used to continuously monitor participants’ actual heart rates in real-time, with Bluetooth communication for data logging. The experimental conditions are provided in Fig. 2

6.3 Procedure

Before the start of the experiment, the participants were briefed about the experimental procedure (both verbally and with instructions on paper). They signed a written consent form to participate in the experiment and provided demographics.

For the experiment, participants stood in a quiet, controlled environment with minimal distractions. They wore headphones and were placed at the location associated with high pressure for the 78 Hz modulation frequency (they stood in the same location for vibrotactile feedback as well). The role of headphones was two-fold. During *Heartbeat Resonance*, the headphones were used to block audible sound from the subwoofer, however, some feedback from the subwoofer was audible despite the headphones. To introduce the same level of audible feedback, the headphones played heartbeat sounds during the vibrotactile feedback (the same sound as the one delivered through the wrist in that trial) to ensure a fair comparison.

Both the delivery mechanisms used the signals described in Section 6.2 to deliver feedback. The wrist-worn vibrotactile motor was not removed for the *Heartbeat Resonance* trials to ensure against confounding effects. The Polar H10 heart rate belt was securely attached to monitor their heart rate throughout the experiment. The stepwise procedure for the experiment is presented in Fig. 8, and detailed as follows:

- (1) **Initial Baseline Period**: Participants sat quietly for 3 minutes without any stimulation to allow their heart rates to stabilize. After this, their baseline heart rate was recorded for 1.5 minutes to ensure that the initial reading reflected a true resting state. The baseline was recorded standing up as

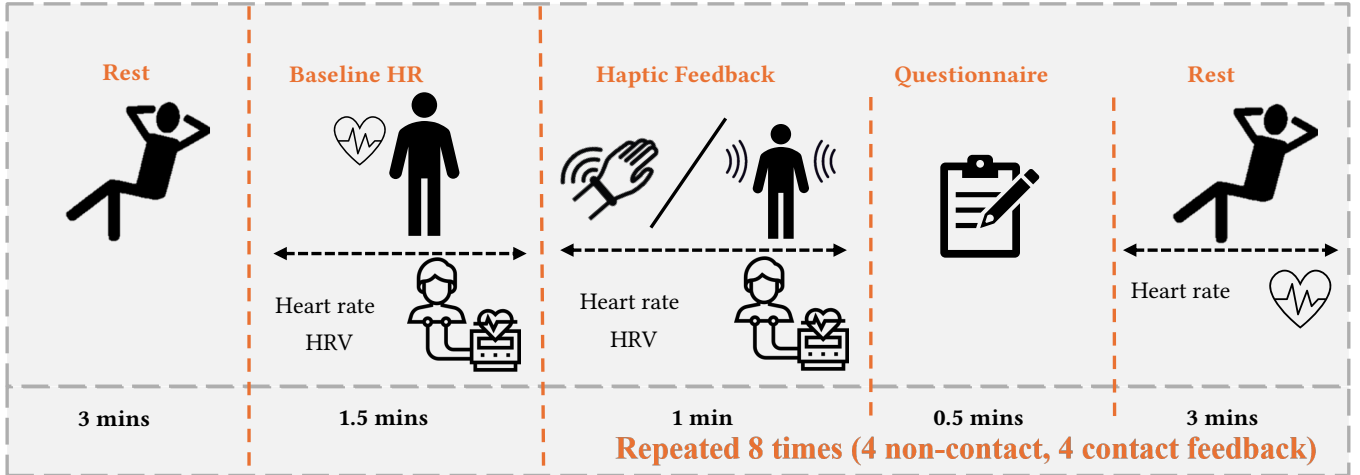


Figure 8: Procedure flowchart for Experiment 2 (Perceived Heart Rate Entrainment). The experiment begins with a 3-minute rest period, followed by a 1.5-minute baseline heart rate (HR) measurement. The core experimental phase is repeated 8 times, consisting of 4 non-contact and 4 contact feedback sessions. Each session includes 1 minute of feedback, 0.5 minutes for answering the questionnaire, and a 3-minute rest period. HR was measured continuously throughout the experiment.

the other conditions (Heartbeat Resonance and Vibrotactile feedback) were also conducted standing up.

(2) **Trial Structure:**

- Each trial began with the delivery of the enhanced heartbeat signals, lasting for 1 minute. The participants were standing up when they received the feedback for both delivery mechanisms.
- Following the stimulation, participants were asked to rate (1) the perceived change in their heart rate, and (2) how confident they were in their rating of perceived heart rate change. They answered on a tablet computer.
- Participants then rested (sat down on a chair) for 3 minutes between trials to allow their heart rate to return to baseline levels.

(3) **Total Session Time:** Each trial consisted of a 1-minute stimulation, a brief rating period, and a 3-minute rest period. Including the initial baseline period, the total time for the experiment was approximately 1 hour per participant ($8 \text{ conditions} \times 5 \text{ minutes per condition} + 10 \text{ minutes for initial baseline and ratings} + 10 \text{ minutes for other overshoots}$).

Participants' heart rates were monitored continuously to ensure that the initial reading was the true baseline and that any fluctuations during the initial baseline period were noted. If participants' heart rates did not stabilize within the first 3 minutes, additional time was allowed before proceeding to the first trial. Additionally, rest periods between trials were monitored to ensure participants' heart rates returned to baseline before starting the next condition. If necessary, the rest periods were extended to achieve this.

6.4 Analysis and Results

Perceived Heart Rate Changes. Participants' subjective perceptions of heart rate changes were recorded for *Heartbeat Resonance* (Fig. 9a) and vibrotactile conditions (Fig. 9b). The best results were

for the *Heartbeat Resonance* at +15% BPM, with 65% of participants reporting an increase in heart rate, matching the intended BPM increase. Similarly, *Heartbeat Resonance* at -30% had 50% participants selecting a decrease in perceived heart rate. By contrast, the vibrotactile conditions showed more varied responses. In the negative vibrotactile conditions (-15% and -30%), responses were randomly distributed across categories. In the positive vibrotactile conditions (+15% and +30%), around half perceived the intended increase, but a significant portion reported no change. While both delivery mechanisms performed well on the positive side (i.e., with BPM increases), *Heartbeat Resonance* had a clear advantage on the negative side.

For further analysis, the conditions were divided into two categories: positive conditions (involving increased heart rates) and negative conditions (involving decreased heart rates). The frequency of each perception response (increase, decrease, same) was calculated for each category.

A Chi-square test revealed a statistically significant difference, $\chi^2(1, N = 160) = 16.94, p < 0.01$ between the positive and negative conditions (combined for both delivery mechanisms). It indicated that participants were more likely to perceive changes in their heart rate in a manner consistent with the direction of the induced changes. In contrast, there was no significant difference between delivery mechanisms (*Heartbeat Resonance* vs. Vibrotactile), $\chi^2(1, N = 160) = 1.85, p = 0.3961$.

Confidence Ratings. The confidence ratings were averaged for each condition. The results of the Friedman test indicated no significant differences in confidence levels across the conditions, $\chi^2(7, N = 18) = 11.89, p = 0.1042$. This suggests that neither the type of feedback (*Heartbeat Resonance* or Vibrotactile) nor the magnitude of BPM variations significantly impacted participants' confidence in their perceptions.

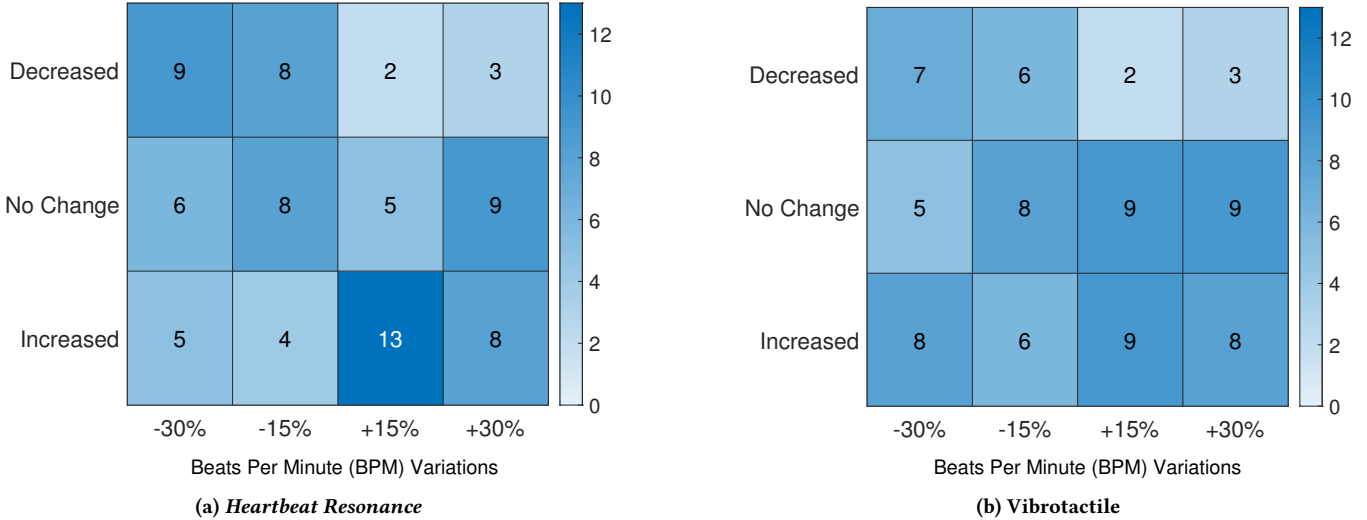


Figure 9: Distribution of perceived heart rate changes across experimental conditions.

To visualize the differences between conditions, we combined the low confidence (1-2) and high confidence (4-5) ratings (excluding the neutral rating of 3). Figure 10 shows the distribution of confidence ratings in perceived change in the heart rate of participants. Overall, participants showed higher confidence in *Heartbeat Resonance*, particularly for the +15% bpm increase and -30% bpm decrease conditions, as shown in Fig. 10a.

Perception With High Confidence. Figure 11 shows the percentage of correct responses categorized by confidence level for the *Heartbeat Resonance* and Vibrotactile conditions. The raw data for correct and incorrect responses is provided in Appendix C.1. However, we relaxed the conditions for counting the incorrect responses. We removed the responses where participants reported “no change” in heart rate (data in Appendix C.2). Including these responses could introduce ambiguity, as they may indicate indecision. Hence, the total count was the one where they either reported an increase or decrease in heart rate with high or low confidence (excluding neutral confidence ratings).

For the *Heartbeat Resonance* condition, the +15% BPM variation exhibited the highest percentage of correct responses, with 66.7% reporting high confidence and an additional 25% reporting low confidence. For the -30% and -15% BPM variations, correct responses with high confidence were 38.5% and 25%, respectively, while the +30% BPM variation showed 57.1% correct responses with high confidence. In the Vibrotactile condition, all the BPM variations showed around 30% of correct responses with high confidence. Whereas the +15% and +30% BPM variation showed an additional 50% and 43% of correct responses with low confidence.

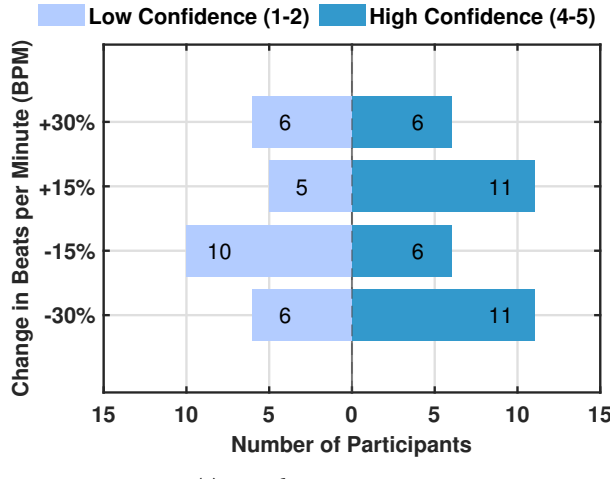
Overall, the *Heartbeat Resonance* conditions (see Fig. 11a) show a higher rate of correct responses compared to the Vibrotactile conditions (see Fig. 11b). However, in both conditions, the proportions of correct responses at most modulation levels were close or below chance, indicating that participants may not have been confidently

accurate across all conditions. The inclusion of low confidence accurate response placed most conditions at a better-than-chance level.

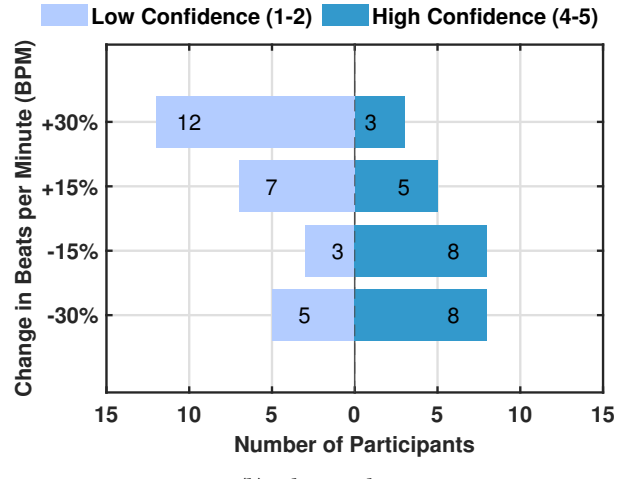
Heart Rate Data. The RR interval data recorded during exposure to the feedback was used to calculate the heart rate and Heart Rate Variability (HRV). Heart rate was calculated using $HR (\text{bpm}) = \frac{60000}{\text{RR interval (ms)}}$, while HRV (RMSSD) was calculated as the difference between RR intervals ($\text{RMSSD} = \sqrt{\frac{1}{n-1} \sum_{i=1}^{n-1} (RR_{i+1} - RR_i)^2}$), where RMSSD is the Root Mean Square of Successive Differences, n is the number of RR intervals, and RR_i is the i -th RR interval. To measure the effect of feedback on participants, we investigated the deviations in heart rate after exposure. The deviations were calculated by comparing the mean heart rate during the feedback duration to the mean heart rate of the resting condition. The mean deviations in heart rate are shown in Fig. 12a and detailed in Appendix C.3. RMSSD was used to assess short-term changes in heart rate, reflecting the body’s ability to regulate heart function through relaxation and recovery. The RMSSD values are presented in Fig. 12b and detailed in Appendix C.4. A paired t-test revealed that the *Heartbeat Resonance* at +15% BPM variation was significantly different from the baseline resting ($p < 0.05$) for heart rate deviations.

7 Discussion

In this study, we demonstrated the effectiveness of *Heartbeat Resonance* in mimicking heartbeat sensations in the chest and facilitating entrainment. The results showed that a modulation frequency of 78.05 Hz produced the most realistic heartbeat sensations (Fig. 4a), while 200.18 Hz produced the most intense sensations (Fig. 4b). These sensations were experienced inside the chest cavity (Fig. 7), particularly on the left side (Fig. 6). *Heartbeat Resonance* induced the perception of heart rate modulation, as reflected by participants’ reported perceived changes and confidence levels (see Figs. 9, 10), and in the +15% BPM variation, this was accompanied by significant

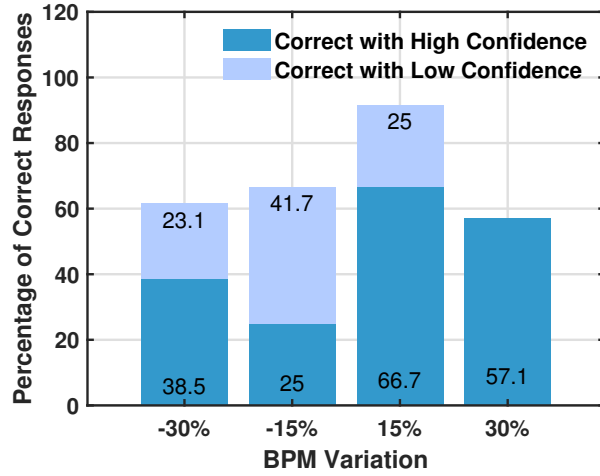


(a) Heartbeat Resonance

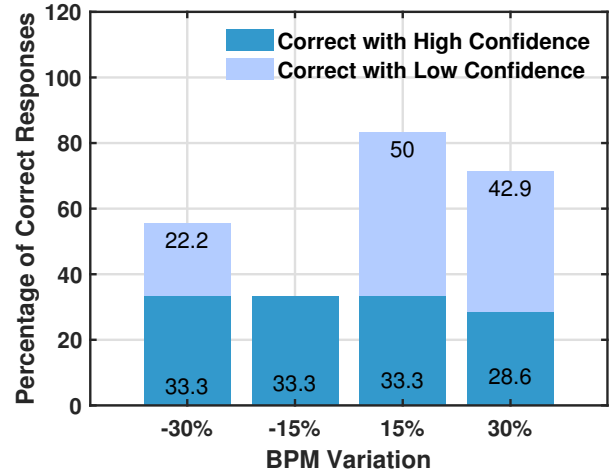


(b) Vibrotactile

Figure 10: The figure illustrates the distribution of participants' confidence ratings, grouped into low confidence (ratings 1-2) and high confidence (ratings 4-5). Neutral responses of 3 are excluded, so the numbers do not sum up to 20 (the number of participants).



(a) Heartbeat Resonance (data in Appendix C.2)



(b) Vibrotactile (data in Appendix Appendix C.2)

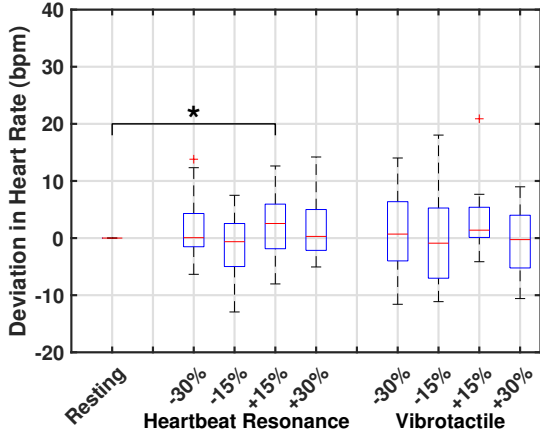
Figure 11: Percentage of correct responses categorized by confidence level for BPM modulation levels in (a) Heartbeat Resonance and (b) Vibrotactile conditions. The bars represent the proportion of correct responses that were given with high confidence (dark blue) and low confidence (light blue). Data is presented as percentages to account for variations in the total count of responses, which differ due to the exclusion of neutral confidence ratings and “no change” perception responses. The values for these figures and incorrect responses are provided in Appendix C.2.

physiological changes. This demonstrates that *Heartbeat Resonance* induced both perceived and, in one case, physiological entrainment.

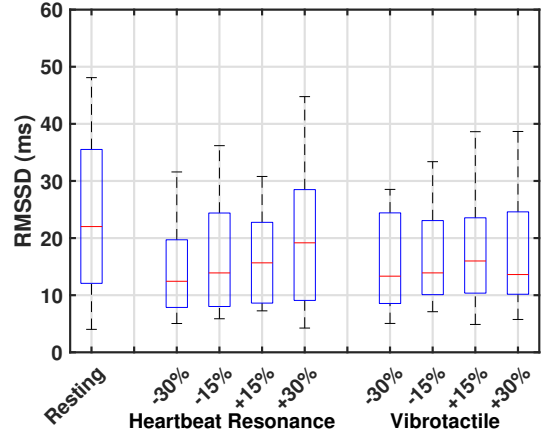
7.1 Most Suitable Theory for Heartbeat Resonance

We look to the theories discussed in Section 2.4 to explain the underlying mechanism for *Heartbeat Resonance*. The effectiveness of these theories is closely linked to the duration and consistency

of exposure to biofeedback. The *Baroreceptor Reflex* can respond almost immediately to simulated changes in heart rate, leading to quick adjustments in cardiovascular function [24]. In contrast, the *Psychophysiological Principle* and *Operant Conditioning* require repeated exposure over time to develop strong connections between physiological signals and psychological states [86], or to reinforce learned behaviors [72], respectively. The *Vagal Afferent Pathways* similarly benefit from prolonged exposure [90], as consistent enhancement of vagal tone is necessary for lasting improvements in



(a) Box plot showing the deviation in heart rate (bpm) across the eight experimental conditions from the baseline condition (resting). The asterisk (*) indicates a significant ($p < 0.05$). Detailed data are provided in Appendix C.3.



(b) Box plot displaying the RMSSD (Root Mean Square of Successive Differences) –time-domain measure of HRV—values across the eight experimental conditions and baseline resting. Detailed data are provided in Appendix C.4.

Figure 12: (a) The heart rate and (b) heart rate variability data recorded during exposure to the experimental conditions.

autonomic regulation. Lastly, *Resonance Frequency Feedback* can yield immediate benefits during each session, but sustained practice is required for long-term improvements in HRV and overall autonomic balance [57].

Given the specific approach of *Heartbeat Resonance*, the most applicable theories are the *Baroreceptor Reflex* and *Vagal Afferent Pathways*. The *Baroreceptor Reflex* is significant as our system directly influences the perceived heartbeat, which can trigger this reflex to regulate the user's actual heart rate. Although physiological changes were rarely observed, the participants' perception of slower or faster heart rates might have influenced this reflex. The *Vagal Afferent Pathways* are also relevant. *Heartbeat Resonance* mimics heartbeats inside the chest which may engage these pathways, helping users experience a greater sense of bodily regulation. However, this theory only explains that HRB increases vagal tone, without addressing how varying the delivered heartbeat sensations (increasing or decreasing) affects outcomes. Among these two, the *Baroreceptor Reflex* likely serves as the primary underlying mechanism due to its effectiveness over short periods. However, the role of other theories cannot be entirely discounted without further research.

7.2 Comparison to Existing Methods

Compared to traditional biofeedback methods, such as wearable vibrotactile devices [61], visual [3], or auditory cues [59], *Heartbeat Resonance* offers an advantage in terms of user comfort and realism. Wearable devices often require direct physical contact, which can be cumbersome or uncomfortable for extended use. Additionally, they often provide feedback in ways that may not feel directly linked to the bodily signal they are meant to simulate, such as delivering vibrations to the finger [98], palm [105], or wrist [14] to represent heartbeats. In contrast, *Heartbeat Resonance* generates heartbeat

sensations directly in the chest, where users expect to feel their heart rate, resulting in a more natural and immersive experience.

However, it is important to note that *Heartbeat Resonance* is restricted to indoor environments due to the need for an acoustically sealed environment and precise positioning. In contrast, wearable vibrotactile devices can be used in any setting, providing greater flexibility for users to receive feedback while on the move or in diverse environments. This portability makes wearable devices more suitable for scenarios where mobility is a key factor.

In Experiment 2 (Perceived Heart Rate Entrainment), we directly compared the non-contact heartbeat sensations generated by *Heartbeat Resonance* with traditional vibrotactile heartbeat feedback delivered through vibrations on the wrist. Figure 9 shows that both methods had comparable results, with *Heartbeat Resonance* slightly outperforming vibrotactile feedback in certain conditions. While vibrotactile feedback was effective, especially in conveying increases in heart rate, *Heartbeat Resonance* provided a more consistent experience overall, particularly when conveying both increases and decreases in heart rate. Participants were also more confident in perceiving their biosignals when *Heartbeat Resonance* was used for feedback.

7.3 Optimal Parameters for *Heartbeat Resonance*

The results of our experiments help us to determine the most effective conditions for delivering realistic heart rate biofeedback using *Heartbeat Resonance*. Specifically, we investigate which modulation frequencies and signal types provided the most accurate and believable heart rate sensations, comparing both non-contact (*Heartbeat Resonance*) and vibrotactile methods.

In Experiment 1 (Inducing Heartbeat Sensations), the 78 Hz modulation frequency demonstrated significantly better realism than the real heartbeat signal (Fig. 5a), while the intensity ratings for

78 Hz, 156 Hz, and 200 Hz were all significantly higher than the real signal (Fig. 5b). However, 78 Hz was particularly effective for localizing sensations to the chest area (Fig. 6), making it the most natural for simulating heartbeats. Additionally, the enhanced heartbeat signal, which included more detailed heartbeat components, was perceived inside the body (or both inside and on the surface) most frequently (Fig. 7). These results led us to choose the *Enhanced Heartbeat Signal* at 78 Hz for Experiment 2 (Perceived Heart Rate Entrainment).

In Experiment 2, we noticed that *Heartbeat Resonance* with +15% BPM increase consistently outperformed *Heartbeat Resonance* with +30% BPM increase, indicating that the +30% increase was perceived as too extreme, while the +15% increase facilitated entrainment and felt more natural. For decreasing heart rates, *Heartbeat Resonance* -30% decrease proved more effective than *Heartbeat Resonance* -15% decrease, indicating that participants required a larger reduction to perceive entrainment of a heart rate decrease. The participants also showed the most confidence in their perception of heart rate changes under the *Heartbeat Resonance* +15% increase and *Heartbeat Resonance* -30% decrease conditions. In summary, we can use the enhanced heartbeat signal modulated at 78 Hz with a linearly increasing BPM up to +15 % of the current heart rate to induce a perception of an increasing heart rate –facilitating entrainment to exhibit excitement. Similarly, the enhanced heartbeat signal modulated at 78 Hz with a linearly decreasing BPM up to -30 % below the current heart rate induces a perception of decreasing heart rate, supporting entrainment to exhibit calm.

7.4 Benefits of Inducing Heartbeat Sensations Inside the Chest Cavity

Inducing heartbeat sensations directly within the chest cavity promotes entrainment and may help enhance interoceptive ability by providing natural feedback sensations. According to the theory of predictive coding [4], the brain forms internal models based on past experiences to interpret incoming sensory information. In the context of heart rate perception, *Heartbeat Resonance* can help people with lower interoceptive ability by providing an external, consistent heartbeat signal that they can use to develop an internal sensory model. For people who are familiar with how their heart feels as it beats (high interoceptive ability), this feedback can further support entrainment and improve synchronization with internal signals [63, 99].

In general, when feedback feels authentic and aligns with how the body usually experiences internal signals, it becomes easier for users to interpret and engage with the information. This principle is well documented in the rubber hand illusion [17]. The authenticity of the illusion increases as the realism of the rubber hands increases [62]. *Heartbeat Resonance* follows the same principle by simulating heartbeats in the chest, the natural location where these sensations are expected to occur. This aligns both the location and feel of the heartbeats with the body's natural sensations. This deeper alignment can potentially help users identify and process their heartbeat signals, leading to a better sensory model of heartbeats.

7.5 Applications

Heartbeat Resonance offers various practical uses. Its non-contact design makes it comfortable to use, providing biofeedback without the need for wearable devices. The system could be adapted for virtual reality, where it could increase the realism and emotional engagement of VR environments. By integrating simulated heart rate feedback into VR training for athletes, users could have a more immersive and interactive experience. The system could be expanded to simulate other bodily signals, like breathing, to increase its effectiveness in a variety of biofeedback scenarios.

Another potential application for *Heartbeat Resonance* is using heartbeats to convey the state of objects, such as electronics, consumables, or degradable materials. The heartbeats could increase or decrease depending on the object's condition, helping users become more aware of environmental or practical concerns. For example, the “heartbeat” of a device could indicate when it's running low on power or approaching failure, creating a more intuitive way to monitor its status.

Similarly, conveying the heartbeats of other people through the system could foster empathy, by allowing individuals to feel one another's physiological state [67, 98]. This could be a unique way to build a sense of connection and emotional understanding in various social or collaborative settings.

7.6 Limitations and Future Work

Limitations: While *Heartbeat Resonance* demonstrated promising results, several limitations need to be addressed. First, the effects were only tested within a specific room. A more robust evaluation would have been to showcase *Heartbeat Resonance* in more than one room. However, that would have been outside the scope of the current project. We plan to evaluate the whole system in new environments in future projects. Second, the room used in our current setup was empty which is not a true reflection of the real world. The simulation code provided in the supplementary material can account for objects in the room (Appendix A.2), specifically large immovable objects. Introducing objects would change the pressure distribution of the standing waves, but the standing waves would exist nevertheless (albeit at a lower pressure or with some noise). In the current system, we kept the room empty to ensure robust standing waves. Additionally, the feedback was tested only for short durations. Although these brief exposures were sufficient to influence perception, they rarely induced measurable changes in heart rate. This limitation prevents us from fully assessing the physiological impact of the feedback in its current form.

Future Work: To address these limitations, future studies will explore the effects of longer exposure times, such as 3 to 5 minutes, to observe whether sustained feedback can lead to more substantial physiological responses. Furthermore, we plan to conduct longitudinal studies to evaluate the long-term benefits of *Heartbeat Resonance*, particularly in enhancing emotional regulation and interoceptive awareness. Another key area for exploration is whether it can improve interoceptive accuracy by helping individuals better recognize and respond to their internal bodily signals. Testing *Heartbeat Resonance*'s effectiveness in these areas will provide a more comprehensive understanding of its potential applications and impact.

8 Conclusion

In this study, we presented *Heartbeat Resonance*, a non-contact feedback system that delivers heartbeat sensations directly inside the chest cavity. By utilizing low-frequency acoustic feedback, it delivers sensations without the need for physical wearables. Through the experiments, we demonstrated that *Heartbeat Resonance* effectively enhances users' perception of heartbeats. In Experiment 1 (Inducing Heartbeat Sensations), we found that the 78 Hz modulation frequency provided the most realistic and localized sensations in the chest. In Experiment 2 (Perceived Heart Rate Entrainment), moderate increases (+15%) and larger decreases (-30%) in heart rate were most effective for entrainment, with participants expressing the highest confidence in these conditions. These findings suggest that *Heartbeat Resonance* could have significant applications in immersive virtual reality environments.

Acknowledgments

This work is funded by the European Union's Horizon 2020 research and innovation programme [grant number 101017746, TOUCHLESS].

References

- [1] Agorastos Agorastos and George P. Chrousos. 2022. The neuroendocrinology of stress: the stress-related continuum of chronic disease development. *Molecular Psychiatry* 27, 1 (2022), 502–513. <https://doi.org/10.1038/s41380-021-01224-9>
- [2] F.Q. AL-Khalidi, R. Saatchi, D. Burke, H. Elphick, and S. Tan. 2011. Respiration rate monitoring methods: A review. *Pediatric Pulmonology* 46, 6 (2011), 523–529. <https://doi.org/10.1002/ppul.21416>
- [3] Hussein Al Osman, Haiwei Dong, and Abdulmotaleb El Saddik. 2016. Ubiquitous Biofeedback Serious Game for Stress Management. *IEEE Access* 4 (2016), 1274–1286. <https://doi.org/10.1109/ACCESS.2016.2548980>
- [4] Matthew A.J. Apps and Manos Tsakiris. 2014. The free-energy self: A predictive coding account of self-recognition. *Neuroscience & Biobehavioral Reviews* 41 (2014), 85–97. <https://doi.org/10.1016/j.neubiorev.2013.01.029> Multisensory integration, sensory substitution and visual rehabilitation.
- [5] Rodger Ashton, Kenneth D White, and Gregory Hodgson. 1979. Sensitivity to heart rate: A psychophysical study. *Psychophysiology* 16, 5 (1979), 463–466. <https://doi.org/10.1111/j.1469-8986.1979.tb01505.x>
- [6] Chiara Baiano, Xavier Job, Gabriella Santangelo, Malika Auvray, and Louise P. Kirsch. 2021. Interactions between interoception and perspective-taking: Current state of research and future directions. *Neuroscience & Biobehavioral Reviews* 130 (2021), 252–262. <https://doi.org/10.1016/j.neubiorev.2021.08.007>
- [7] Sandhya Basu and Bidisha Banerjee. 2020. Prospect of Brainwave Entrainment to Promote Well-Being in Individuals: A Brief Review. *Psychological Studies* 65, 3 (2020), 296–306. <https://doi.org/10.1007/s12646-020-00555-x>
- [8] Luciano Bernardi, Cesare Porta, Gaia Casucci, Rossella Balsamo, Nicolò F. Bernardi, Roberto Fogari, and Peter Sleight. 2009. Dynamic Interactions Between Musical, Cardiovascular, and Cerebral Rhythms in Humans. *Circulation* 119, 25 (2009), 3171–3180. <https://doi.org/10.1161/CIRCULATIONAHA.108.806174>
- [9] Jim Blascovich and Wendy Berry Mendes. 2010. Social psychophysiology and embodiment. *Handbook of social psychology* 1 (2010), 194–227.
- [10] Johannes Blum, Christoph Rockstroh, and Anja S. Göritz. 2020. Development and Pilot Test of a Virtual Reality Respiratory Biofeedback Approach. *Applied Psychophysiology and Biofeedback* 45, 3 (2020), 153–163. <https://doi.org/10.1007/s10484-020-09468-x>
- [11] Bruno Bonaz, Richard D. Lane, Michael L. Oshinsky, Paul J. Kenny, Rajita Sinha, Emeran A. Mayer, and Hugo D. Critchley. 2021. Diseases, Disorders, and Comorbidities of Interoception. *Trends in Neurosciences* 44, 1 (2021), 39–51. <https://doi.org/10.1016/j.tins.2020.09.009> Special Issue: The Neuroscience of Interoception.
- [12] Joseph N. Cappella. 1997. Behavioral and judged coordination in adult informal social interactions: Vocal and kinesic indicators. *Journal of Personality and Social Psychology* 72, 1 (1997), 119–131. <https://doi.org/10.1037/0022-3514.72.1.119>
- [13] Wen G Chen, Dana Schloesser, Angela M Arendorf, Janine M Simmons, Chang-hai Cui, Rita Valentino, James W Gnadt, Lisbeth Nielsen, Coryse St Hillaire-Clarke, Victoria Spruance, et al. 2021. The emerging science of interoception: sensing, integrating, interpreting, and regulating signals within the self. *Trends in neurosciences* 44, 1 (2021), 3–16. <https://doi.org/10.1016/j.tins.2020.10.007>
- [14] Kyung Yun Choi and Hiroshi Ishii. 2020. ambienBeat: Wrist-worn Mobile Tactile Biofeedback for Heart Rate Rhythmic Regulation. In *Proceedings of the Fourteenth International Conference on Tangible, Embedded, and Embodied Interaction* (Sydney NSW, Australia) (TEI '20). Association for Computing Machinery, New York, NY, USA, 17–30. <https://doi.org/10.1145/3374920.3374938>
- [15] Jean Costa, Alexander T. Adams, Malte F. Jung, François Guimbretière, and Tanzeem Choudhury. 2016. EmotionCheck: leveraging bodily signals and false feedback to regulate our emotions. In *Proceedings of the 2016 ACM International Joint Conference on Pervasive and Ubiquitous Computing* (Heidelberg, Germany) (UbiComp '16). Association for Computing Machinery, New York, NY, USA, 758–769. <https://doi.org/10.1145/2971648.2971752>
- [16] Jean Costa, François Guimbretière, Malte F. Jung, and Tanzeem Choudhury. 2019. BoostMeUp: Improving Cognitive Performance in the Moment by Unobtrusively Regulating Emotions with a Smartwatch. *Proc. ACM Interact. Mob. Wearable Ubiquitous Technol.* 3, 2, Article 40 (2019), 23 pages. <https://doi.org/10.1145/3328911>
- [17] Marcello Costantini and Patrick Haggard. 2007. The rubber hand illusion: Sensitivity and reference frame for body ownership. *Consciousness and Cognition* 16, 2 (2007), 229–240. <https://doi.org/10.1016/j.concog.2007.01.001>
- [18] Pilar Cristancho, Mario A Cristancho, Gordon H Baltuch, Michael E Thase, PO John, et al. 2011. Effectiveness and safety of vagus nerve stimulation for severe treatment-resistant major depression in clinical practice after FDA approval: outcomes at 1 year. *The journal of clinical psychiatry* 72, 10 (2011), 5594. <https://doi.org/10.4088/JCP.09m0588blu>
- [19] Franco Curmi, Maria Angela Ferrario, Jen Southern, and Jon Whittle. 2013. HeartLink: open broadcast of live biometric data to social networks. In *Proceedings of the SIGCHI Conference on Human Factors in Computing Systems* (Paris, France) (CHI '13). Association for Computing Machinery, New York, NY, USA, 1749–1758. <https://doi.org/10.1145/2470654.2466231>
- [20] Arindam Dey, Hao Chen, Mark Billinghurst, and Robert W. Lindeman. 2018. Effects of Manipulating Physiological Feedback in Immersive Virtual Environments. In *Proceedings of the 2018 Annual Symposium on Computer-Human Interaction in Play* (Melbourne, VIC, Australia) (CHI PLAY '18). Association for Computing Machinery, New York, NY, USA, 101–111. <https://doi.org/10.1145/3242671.3242676>
- [21] Olga Dobrushina, Yossi Tamim, Iddo Yehoshua Wald, Amber Maimon, and Amir Amedi. 2024. Interceptive training with real-time haptic versus visual heartbeat feedback. *Psychophysiology* (2024), e14648. <https://doi.org/10.1111/psyp.14648>
- [22] Aidan D'Souza, Bernd Ploderer, Madison Klarkowski, and Peta Wyeth. 2018. Augmenting Co-Located Social Play with Biofeedback: An Interactional Approach. In *Proceedings of the 2018 Annual Symposium on Computer-Human Interaction in Play* (Melbourne, VIC, Australia) (CHI PLAY '18). Association for Computing Machinery, New York, NY, USA, 113–125. <https://doi.org/10.1145/3242671.3242679>
- [23] Barnaby D Dunn, Iolanta Stefanovitch, Davy Evans, Clare Oliver, Amy Hawkins, and Tim Dalgleish. 2010. Can you feel the beat? Interoceptive awareness is an interactive function of anxiety-and depression-specific symptom dimensions. *Behaviour research and therapy* 48, 11 (2010), 1133–1138. <https://doi.org/10.1016/j.brat.2010.07.006>
- [24] Dawin L Eckberg and Peter Sleight. 1992. *Human Baroreflexes in Health and Disease*. Oxford University Press. <https://doi.org/10.1093/oso/9780198576938.001.0001>
- [25] Abdallah El Ali, Rayna Ney, Zeph M. C. van Berlo, and Pablo Cesar. 2023. Is that My Heartbeat? Measuring and Understanding Modality-Dependent Cardiac Interoception in Virtual Reality. *IEEE Transactions on Visualization and Computer Graphics* 29, 11 (2023), 4805–4815. <https://doi.org/10.1109/TVCG.2023.3320228>
- [26] Jorina Elbers and Rollin McCraty. 2020. HeartMath approach to self-regulation and psychosocial well-being. *Journal of Psychology in Africa* 30, 1 (2020), 69–79. <https://doi.org/10.1080/14330237.2020.1712797>
- [27] Bernard T Engel and Ray A Chism. 1967. Operant conditioning of heart rate speeding. *Psychophysiology* 3, 4 (1967), 418–426. <https://doi.org/10.1111/j.1469-8986.1967.tb02728.x>
- [28] Bernard T Engel and Stephen P Hansen. 1966. Operant conditioning of heart rate slowing. *Psychophysiology* 3, 2 (1966), 176–187. <https://doi.org/10.1111/j.1469-8986.1966.tb02693.x>
- [29] BT Engely and M Talan. 2022. Operant conditioning of the cardiovascular adjustments to exercise. In *Perspectives on Research in Emotional Stress*. Routledge, 353–366. <https://doi.org/10.4324/9781315075488-30>
- [30] Paula C. Salamone et. al. 2021. Interoception Primes Emotional Processing: Multimodal Evidence from Neurodegeneration. *Journal of Neuroscience* 41, 19 (2021), 4276–4292. <https://doi.org/10.1523/JNEUROSCI.2578-20.2021>
- [31] Sahib S. Khalsa et. al. 2018. Interoception and Mental Health: A Roadmap. *Biological Psychiatry: Cognitive Neuroscience and Neuroimaging* 3, 6 (2018), 501–513. <https://doi.org/10.1016/j.bpsc.2017.12.004> Interoception and Mental Health.
- [32] Stephen H. Fairclough. 2008. Fundamentals of physiological computing. *Interacting with Computers* 21, 1-2 (11 2008), 133–145. <https://doi.org/10.1016/j.intcom.2008.10.011>
- [33] Cathy Mengying Fang, G. R. Marvez, Neska ElHaouij, and Rosalind Picard. 2022. Cardiac Arrest: Evaluating the Role of Biosignals in Gameplay Strategies

- and Players' Physiological Synchrony in Social Deception Games. In *Extended Abstracts of the 2022 CHI Conference on Human Factors in Computing Systems* (New Orleans, LA, USA) (CHI EA '22). Association for Computing Machinery, New York, NY, USA, Article 240, 7 pages. <https://doi.org/10.1145/3491101.3519670>
- [34] S.J. Farlow. 2012. *Partial Differential Equations for Scientists and Engineers*. Dover Publications. https://books.google.co.kr/books?id=VsK_31_j0XgC
- [35] Dana Fischer, Matthias Messner, and Olga Pollatos. 2017. Improvement of Interoceptive Processes after an 8-Week Body Scan Intervention. *Frontiers in Human Neuroscience* 11 (2017). <https://doi.org/10.3389/fnhum.2017.00452>
- [36] Waka Fujisaki and Shin'ya Nishida. 2009. Audio-tactile superiority over visuo-tactile and audio-visual combinations in the temporal resolution of synchrony perception. *Experimental brain research* 198 (2009), 245–259. <https://doi.org/10.1007/s00221-009-1870-x>
- [37] Sarah N. Garfinkel, André Schulz, and Manos Tsakiris. 2022. Addressing the need for new interoceptive methods. *Biological Psychology* 170 (2022), 108322. <https://doi.org/10.1016/j.biopsych.2022.108322>
- [38] Sarah N. Garfinkel, Anil K. Seth, Adam B. Barrett, Keisuke Suzuki, and Hugo D. Critchley. 2015. Knowing your own heart: Distinguishing interoceptive accuracy from interoceptive awareness. *Biological Psychology* 104 (2015), 65–74. <https://doi.org/10.1016/j.biopsych.2014.11.004>
- [39] Renaud Gervais, Jérémie Frey, Alexis Gay, Fabien Lotte, and Martin Hachet. 2016. TOBE: Tangible Out-of-Body Experience. In *Proceedings of the TEI '16: Tenth International Conference on Tangible, Embedded, and Embodied Interaction* (Eindhoven, Netherlands) (TEI '16). Association for Computing Machinery, New York, NY, USA, 227–235. <https://doi.org/10.1145/2839462.2839486>
- [40] V. C. Goessl, J. E. Curtiss, and S. G. Hofmann. 2017. The effect of heart rate variability biofeedback training on stress and anxiety: a meta-analysis. *Psychological Medicine* 47, 15 (2017), 2578–2586. <https://doi.org/10.1017/S0033291717001003>
- [41] Jeffrey L. Goodie and Kevin T. Larkin. 2006. Transfer of Heart Rate Feedback Training to Reduce Heart Rate Response to Laboratory Tasks. *Applied Psychophysiology and Biofeedback* 31, 3 (2006), 227–242. <https://doi.org/10.1007/s10484-006-9011-9>
- [42] Olivia K Harrison, Laura Köchli, Stephanie Marino, Roger Luechinger, Franciszek Henzel, Katja Brand, Alexander J Hess, Stefan Frässle, Sandra Iglesias, Fabien Vinckier et al. 2021. Interoception of breathing and its relationship with anxiety. *Neuron* 109, 24 (2021), 4080–4093. <https://doi.org/10.1016/j.neuron.2021.09.045>
- [43] Waaseem Hassan, Aiser Marzo, and Kasper Hornbæk. 2024. Using Low-frequency Sound to Create Non-contact Sensations On and In the Body. In *Proceedings of the CHI Conference on Human Factors in Computing Systems* (Honolulu, HI, USA) (CHI '24). Association for Computing Machinery, New York, NY, USA, Article 887, 22 pages. <https://doi.org/10.1145/3613904.3642311>
- [44] Mariam Hassib, Daniel Buschek, Paweł W. Woźniak, and Florian Alt. 2017. HeartChat: Heart Rate Augmented Mobile Chat to Support Empathy and Awareness. In *Proceedings of the 2017 CHI Conference on Human Factors in Computing Systems* (Denver, Colorado, USA) (CHI '17). Association for Computing Machinery, New York, NY, USA, 2239–2251. <https://doi.org/10.1145/3025453.3025758>
- [45] Beate M Herbert, Cornelius Herbert, and Olga Pollatos. 2011. On the relationship between interoceptive awareness and alexithymia: is interoceptive awareness related to emotional awareness? *Journal of personality* 79, 5 (2011), 1149–1175. <https://doi.org/10.1111/j.1467-6494.2011.00717.x>
- [46] Noura Howell, Greg Niemeyer, and Kimiko Ryokai. 2019. Life-Affirming Biosensing in Public: Soundings Heartbeats on a Red Bench. In *Proceedings of the 2019 CHI Conference on Human Factors in Computing Systems* (Glasgow, Scotland Uk) (CHI '19). Association for Computing Machinery, New York, NY, USA, 1–16. <https://doi.org/10.1145/3290605.3300910>
- [47] Giulio Jacucci, Stephen Fairclough, and Erin T. Solovey. 2015. Physiological Computing. *Computer* 48, 10 (2015), 12–16. <https://doi.org/10.1109/MC.2015.291>
- [48] Paul M. Jenkinson, Aikaterini Fotopoulou, Agustín Ibañez, and Susan Rossell. 2024. Interoception in anxiety, depression, and psychosis: a review. *eClinicalMedicine* 73 (2024), 102673. <https://doi.org/10.1016/j.eclinm.2024.102673>
- [49] Katerina V.-A. Johnson and Laura Steenbergen. 2022. Gut Feelings: Vagal Stimulation Reduces Emotional Biases. *Neuroscience* 494 (2022), 119–131. <https://doi.org/10.1016/j.neuroscience.2022.04.026>
- [50] Sahib S Khalsa, David Rudrauf, Justin S Feinstein, and Daniel Tranel. 2009. The pathways of interoceptive awareness. *Nature neuroscience* 12, 12 (2009), 1494–1496.
- [51] Katherine Knauth, Alexander Waldron, Mishali Mathur, and Vrinda Kalia. 2021. Perceived chronic stress influences the effect of acute stress on cognitive flexibility. *Scientific Reports* 11, 1 (2021), 23629. <https://doi.org/10.1038/s41598-021-03101-5>
- [52] Jean-Philippe Krieger, Mohammed Asker, Pauline van der Velden, Stina Börchers, Jennifer E. Richard, Ivana Maric, Francesco Longo, Arashdeep Singh, Guillaume de Lartigue, and Karolina P. Skibicka. 2022. Neural Pathway for Gut Feelings: Vagal Interoceptive Feedback From the Gastrointestinal Tract Is a Critical Modulator of Anxiety-like Behavior. *Biological Psychiatry* 92, 9 (2022), 709–721. <https://doi.org/10.1016/j.biopsych.2022.04.020> Threat, Stress, and Health.
- [53] S. Laborde, M. S. Allen, U. Borges, M. Iskra, N. Zammit, M. You, T. Hosang, E. Mosley, and F. Dosseville. 2021. Psychophysiological effects of slow-paced breathing at six cycles per minute with or without heart rate variability biofeedback. *Psychophysiology* 59, 1 (2021), e13952. <https://doi.org/10.1111/psyp.13952>
- [54] Kevin T. Larkin, Claudia Zayfert, Jennifer L. Abel, and Lois G. Veltum. 1992. Reducing Heart Rate Reactivity to Stress with Feedback Generalization Across Task and Time. *Behavior Modification* 16, 1 (1992), 118–131. <https://doi.org/10.1177/01454455920161006> PMID: 1540120.
- [55] Paul Lehrer, Karenjo Kaur, Agratta Sharma, Khushbu Shah, Robert Huseby, Jay Bhavsar, Phillip Sgobba, and Yingting Zhang. 2020. Heart Rate Variability Biofeedback Improves Emotional and Physical Health and Performance: A Systematic Review and Meta Analysis. *Applied Psychophysiology and Biofeedback* 45, 3 (2020), 109–129. <https://doi.org/10.1007/s10484-020-09466-z>
- [56] Paul M. Lehrer and Richard Gevirtz. 2014. Heart Rate Variability Biofeedback: How and Why Does It Work? *Frontiers in Psychology* 5 (2014), 756. <https://doi.org/10.3389/fpsyg.2014.00756>
- [57] Paul M. Lehrer, Evgeny Vaschillo, and Bronya Vaschillo. 2000. Resonant Frequency Biofeedback Training to Increase Cardiac Variability: Rationale and Manual for Training. *Applied Psychophysiology and Biofeedback* 25, 3 (2000), 177–191. <https://doi.org/10.1023/A:1009554825745>
- [58] Paul M. Lehrer, Evgeny Vaschillo, Bronya Vaschillo, Shou-En Lu, Anthony Scardella, Mahmood Siddique, and Robert H. Habib. 2004. Biofeedback Treatment for Asthma. *Chest* 126, 2 (2004), 352–361. <https://doi.org/10.1378/chest.126.2.352>
- [59] Grace Leslie, Asma Ghandeharioun, Diane Zhou, and Rosalind W. Picard. 2019. Engineering Music to Slow Breathing and Invite Relaxed Physiology. In *2019 8th International Conference on Affective Computing and Intelligent Interaction (ACII)*, 1–7. <https://doi.org/10.1109/ACII.2019.8925531>
- [60] Guiping Lin, Qiuiling Xiang, Xiaodong Fu, Shuzhen Wang, Sheng Wang, Si-juan Chen, Li Shao, Yan Zhao, and Tinghuai Wang. 2012. Heart Rate Variability Biofeedback Decreases Blood Pressure in Prehypertensive Subjects by Improving Autonomic Function and Baroreflex. *The Journal of Alternative and Complementary Medicine* 18, 2 (2012), 143–152. <https://doi.org/10.1089/acm.2010.0607> PMID: 2239103.
- [61] Jiayi Ling, Jing-Chen Hong, Yuki Hayashi, Kazuhiro Yasuda, Yu Kitaji, Hiroaki Harashima, and Hiroyasu Iwata. 2020. A Haptic-Based Perception-Empathy Biofeedback System with Vibration Transition: Verifying the Attention Amount. In *2020 42nd Annual International Conference of the IEEE Engineering in Medicine and Biology Society (EMBC)*, 3779–3782. <https://doi.org/10.1109/EMBC44109.2020.9176213>
- [62] Marilia Lira, Julia H. Egito, Patricia A. Dall'Agnol, David M. Amodio, Óscar F. Gonçalves, and Paulo S. Boggio. 2017. The influence of skin color on the experience of ownership in the rubber hand illusion. *Scientific Reports* 7, 1 (2017), 15745. <https://doi.org/10.1038/s41598-017-16137-3>
- [63] Alexander Lischke, Rike Pahnke, Anett Mau-Möller, and Matthias Weipert. 2021. Heart Rate Variability Modulates Interoceptive Accuracy. *Frontiers in Neuroscience* 14 (2021). <https://doi.org/10.3389/fnins.2020.612445>
- [64] Fannie Liu, Laura Dabbish, and Geoff Kaufman. 2017. Supporting Social Interactions with an Expressive Heart Rate Sharing Application. *Proc. ACM Interact. Mob. Wearable Ubiquitous Technol.* 1, 3, Article 77 (sep 2017), 26 pages. <https://doi.org/10.1145/3130943>
- [65] Fannie Liu, Mario Esparza, María Pavlovská, Geoff Kaufman, Laura Dabbish, and Andrés Monroy-Hernández. 2019. Animo: Sharing Biosignals on a Smartwatch for Lightweight Social Connection. *Proc. ACM Interact. Mob. Wearable Ubiquitous Technol.* 3, 1, Article 18 (mar 2019), 19 pages. <https://doi.org/10.1145/3314405>
- [66] Fannie Liu, Geoff Kaufman, and Laura Dabbish. 2019. The Effect of Expressive Biosignals on Empathy and Closeness for a Stigmatized Group Member. *3, CSCW*, Article 201 (Nov 2019), 17 pages. <https://doi.org/10.1145/3359303>
- [67] Gilad Lotan and Christian Croft. 2007. imPulse. In *CHI '07 Extended Abstracts on Human Factors in Computing Systems* (San Jose, CA, USA) (CHI EA '07). Association for Computing Machinery, New York, NY, USA, 1983–1988. <https://doi.org/10.1145/1240866.1240936>
- [68] Ewa Lux, Marc TP Adam, Verena Dorner, Sina Helming, Michael T Kneirum, and Christof Weinhardt. 2018. Live biofeedback as a user interface design element: A review of the literature. *Communications of the Association for Information Systems* 43, 1 (2018), 18. <https://doi.org/10.17705/1CAIS.04318>
- [69] Georgios Marentakis, Debanjan Borthakur, Paul Batchelor, Judith P. Andersen, and Victoria Grace. 2021. Using Breath-like Cues for Guided Breathing. In *Extended Abstracts of the 2021 CHI Conference on Human Factors in Computing Systems* (Yokohama, Japan) (CHI EA '21). Association for Computing Machinery, New York, NY, USA, Article 468, 7 pages. <https://doi.org/10.1145/3411763.3451796>
- [70] Nick Merrill and Coye Cheshire. 2016. Habits of the Heart(rate): Social Interpretation of Biosignals in Two Interaction Contexts. In *Proceedings of the 2016 ACM International Conference on Supporting Group Work* (Sanibel Island, Florida, USA) (GROUP '16). Association for Computing Machinery, New York, NY, USA, 31–38. <https://doi.org/10.1145/2957276.2957313>

- [71] Nick Merrill and Coye Cheshire. 2017. Trust Your Heart: Assessing Cooperation and Trust with Biosignals in Computer-Mediated Interactions. In *Proceedings of the 2017 ACM Conference on Computer Supported Cooperative Work and Social Computing* (Portland, Oregon, USA) (CSCW '17). Association for Computing Machinery, New York, NY, USA, 2–12. <https://doi.org/10.1145/2998181.2998286>
- [72] Neal E. Miller. 1969. Learning of Visceral and Glandular Responses. *Science* 163, 3866 (1969), 434–445. <https://doi.org/10.1126/science.163.3866.434>
- [73] Nathan Miner, Amir Abdollahi, Caleb Myers, Mehmet Kosa, Hamid Ghadnia, Joseph H. Schwab, Casper Harteveld, and Giovanni Maria Troiano. 2024. Stairway to Heaven: A Gamified VR Journey for Breath Awareness. In *Proceedings of the CHI Conference on Human Factors in Computing Systems* (Honolulu, HI, USA) (CHI '24). Association for Computing Machinery, New York, NY, USA, Article 717, 19 pages. <https://doi.org/10.1145/3613904.3641986>
- [74] Henrik Møller and Christian Sejer Pedersen. 2004. Hearing at low and infrasonic frequencies. *Noise & health* 6, 23 (2004), 37–57. https://journals.lww.com/nohe/fulltext/2004/06230/hearing_at_low_and_infrasonic_frequencies.aspx
- [75] Neema Moraveji, Ben Olson, Truc Nguyen, Mahmoud Saadat, Yaser Khalighi, Roy Pea, and Jeffrey Heer. 2011. Peripheral paced respiration: influencing user physiology during information work. In *Proceedings of the 24th Annual ACM Symposium on User Interface Software and Technology* (Santa Barbara, California, USA) (UIST '11). Association for Computing Machinery, New York, NY, USA, 423–428. <https://doi.org/10.1145/2047196.2047250>
- [76] Matthew Mosher. 2022. Khong Khrö: Visual biofeedback for focus meditations: Visual biofeedback for focus meditations. In *Proceedings of the 14th Conference on Creativity and Cognition* (Venice, Italy) (C&C '22). Association for Computing Machinery, New York, NY, USA, 570–574. <https://doi.org/10.1145/3527927.3535216>
- [77] Abubakr Mustafa, Mazin Yassin, and Ashraf Mahroos. 2017. Patient-Friendly Visual Rehabilitation EMG Biofeedback with TENS Pain Relief Module based on Android Platform. In *Proceedings of the 6th International Conference on Bioinformatics and Biomedical Science* (Singapore, Singapore) (ICBBS '17). Association for Computing Machinery, New York, NY, USA, 152–157. <https://doi.org/10.1145/3121138.3121198>
- [78] Nadine Neukirch, Sophie Reid, and Alice Shires. 2019. Yoga for PTSD and the role of interoceptive awareness: A preliminary mixed-methods case series study. *European Journal of Trauma and Dissociation* 3, 1 (2019), 7–15.
- [79] Minami Noda, Yoko Sato, Yoshiko Suetsugu, and Seiichi Morokuma. 2022. Interoception is associated with anxiety and depression in pregnant women: A pilot study. *Plos one* 17, 5 (2022), e0267507. <https://doi.org/10.1371/journal.pone.0267507>
- [80] Shamoona Noushad, Sadaf Ahmed, Basit Ansari, Umme-Hani Mustafa, Yusra Saleem, and Hina Hazrat. 2021. Physiological biomarkers of chronic stress: A systematic review. *International Journal of Health Sciences* 15, 5 (Sep-Oct 2021), 46–59. <https://www.ncbi.nlm.nih.gov/pmc/articles/PMC8434839/>
- [81] Elisabetta Patron, Simone Messerotti Benvenuti, Giuseppe Favretto, Carlo Valfrè, Carlotta Bonfà, Renata Gasparotto, and Daniela Palomba. 2013. Biofeedback Assisted Control of Respiratory Sinus Arrhythmia as a Biobehavioral Intervention for Depressive Symptoms in Patients After Cardiac Surgery: A Preliminary Study. *Applied Psychophysiology and Biofeedback* 38, 1 (2013), 1–9. <https://doi.org/10.1007/s10484-012-9202-5>
- [82] Nathalie Peira, Mats Fredrikson, and Gilles Pourtois. 2014. Controlling the emotional heart: Heart rate biofeedback improves cardiac control during emotional reactions. *International Journal of Psychophysiology* 91, 3 (2014), 225–231. <https://doi.org/10.1016/j.ijpsycho.2013.12.008>
- [83] Olga Pollatos, Eva Traut-Mattausch, Heike Schroeder, and Rainer Schandry. 2007. Interoceptive awareness mediates the relationship between anxiety and the intensity of unpleasant feelings. *Journal of anxiety disorders* 21, 7 (2007), 931–943. <https://doi.org/10.1016/j.jeад.2018.10.003>
- [84] Rainer Schandry and Rolf Weitkunat. 1990. Enhancement of heartbeat-related brain potentials through cardiac awareness training. *International Journal of Neuroscience* 53, 2–4 (1990), 243–253. <https://doi.org/10.3109/00207459008986611>
- [85] M. H. Schein, B. Gavish, M. Herz, D. Rosner-Kahanah, P. Naveh, B. Knishkowy, E. Zlotnikov, N. Ben-Zvi, and R. N. Melmed. 2001. Treating hypertension with a device that slows and regularises breathing: a randomised, double-blind controlled study. *Journal of Human Hypertension* 15, 4 (2001), 271–278. <https://doi.org/10.1038/sj.jhh.1001148>
- [86] Gary E. Schwartz. 1975. Biofeedback, Self-Regulation, and the Patterning of Physiological Processes: By training subjects to control voluntarily combinations of visceral, neural, and motor responses, it is possible to assess linkages between physiological responses and their relationship to human consciousness. *American Scientist* 63, 3 (1975), 314–324. <http://www.jstor.org/stable/27845467>
- [87] M.S. Schwartz and F. Andrasik. 2017. *Biofeedback, Fourth Edition: A Practitioner's Guide*. Guilford Publications. <https://books.google.co.kr/books?id=mqgHDgAAQBAJ>
- [88] Petr Slovák, Joris Janssen, and Geraldine Fitzpatrick. 2012. Understanding heart rate sharing: towards unpacking physiosocial space. In *Proceedings of the SIGCHI Conference on Human Factors in Computing Systems* (Austin, Texas, USA) (CHI '12). Association for Computing Machinery, New York, NY, USA, 859–868. <https://doi.org/10.1145/2207676.2208526>
- [89] Jaime Snyder, Mark Matthews, Jacqueline Chien, Pamara F. Chang, Emily Sun, Saeed Abdullah, and Geri Gay. 2015. MoodLight: Exploring Personal and Social Implications of Ambient Display of Biosensor Data (CSCW '15). Association for Computing Machinery, New York, NY, USA, 143–153. <https://doi.org/10.1145/2675133.2675191>
- [90] Julian F. Thayer and Richard D. Lane. 2009. Claude Bernard and the heart–brain connection: Further elaboration of a model of neurovisceral integration. *Neuroscience and Biobehavioral Reviews* 33, 2 (2009), 81–88. <https://doi.org/10.1016/j.neubiorev.2008.08.004> The Inevitable Link between Heart and Behavior: New Insights from Biomedical Research and Implications for Clinical Practice.
- [91] Dzmitry Tsetserukou, Alena Neviarouskaya, Helmut Prendinger, Naoki Kawakami, and Susumu Tachi. 2009. Affective haptics in emotional communication. In *2009 3rd International Conference on Affective Computing and Intelligent Interaction and Workshops*. 1–6. <https://doi.org/10.1109/ACII.2009.5349516>
- [92] Andreia Valente, Dajin Lee, Seungmoon Choi, Mark Billinghurst, and Augusto Esteves. 2024. Modulating Heart Activity and Task Performance using Haptic Heartbeat Feedback: A Study Across Four Body Placements. In *Proceedings of the 37th Annual ACM Symposium on User Interface Software and Technology* (Pittsburgh, PA, USA) (UIST '24). Association for Computing Machinery, New York, NY, USA, Article 25, 13 pages. <https://doi.org/10.1145/3654777.3676435>
- [93] Juan Antonio Valera-Calero, César Fernández-de-las Peñas, Umut Varol, Ricardo Ortega-Santiago, Gracia María Gallego-Sendarrubias, and José Luis Arias-Buría. 2021. Ultrasound Imaging as a Visual Biofeedback Tool in Rehabilitation: An Updated Systematic Review. *International Journal of Environmental Research and Public Health* 18, 14 (2021). <https://doi.org/10.3390/ijerph18147554>
- [94] Evgeny G. Vaschillo, Bronya Vaschillo, and Paul M. Lehrer. 2006. Characteristics of Resonance in Heart Rate Variability Stimulated by Biofeedback. *Applied Psychophysiology and Biofeedback* 31, 2 (2006), 129–142. <https://doi.org/10.1007/s10484-006-9009-3>
- [95] Nicolas Vuillerme, Olivier Chenu, Jacques Demangeot, and Yohan Payan. 2007. Controlling posture using a plantar pressure-based, tongue-placed tactile biofeedback system. *Experimental brain research* 179 (2007), 409–414. <https://doi.org/10.1007/s00221-006-0800-4>
- [96] Nicolas Vuillerme, Nicolas Pinsault, Olivier Chenu, Anthony Fleury, Yohan Payan, and Jacques Demangeot. 2009. A wireless embedded tongue tactile biofeedback system for balance control. *Pervasive and Mobile Computing* 5, 3 (2009), 268–275. <https://doi.org/10.1016/j.pmcj.2008.04.001>
- [97] Ruoxi Wang, Haifeng Zhang, Shauna Alexander Macdonald, and Patrizia Di Campli San Vito. 2023. Increasing Heart Rate and Anxiety Level with Vibrotactile and Audio Presentation of Fast Heartbeat. In *Proceedings of the 25th International Conference on Multimodal Interaction* (Paris, France) (ICMI '23). Association for Computing Machinery, New York, NY, USA, 355–363. <https://doi.org/10.1145/3577190.3614161>
- [98] Julia Werner, Reto Wettach, and Eva Hornecker. 2008. United-pulse: feeling your partner's pulse. In *Proceedings of the 10th International Conference on Human Computer Interaction with Mobile Devices and Services* (Amsterdam, The Netherlands) (MobileHCI '08). Association for Computing Machinery, New York, NY, USA, 535–538. <https://doi.org/10.1145/1409240.1409338>
- [99] Natalie S. Werner, Stefan Duschek, Michael Mattern, and Rainer Schandry. 2009. Interoceptive Sensitivity Modulates Anxiety During Public Speaking. *Journal of Psychophysiology* 23, 2 (2009), 85–94. <https://doi.org/10.1027/0269-8803.23.2.85>
- [100] Udo Will and Eric Berg. 2007. Brain wave synchronization and entrainment to periodic acoustic stimuli. *Neuroscience Letters* 424, 1 (2007), 55–60. <https://doi.org/10.1016/j.neulet.2007.07.036>
- [101] R. Michael Winters, Bruce N. Walker, and Grace Leslie. 2021. Can You Hear My Heartbeat?: Hearing an Expressive Biosignal Elicits Empathy. In *Proceedings of the 2021 CHI Conference on Human Factors in Computing Systems* (Yokohama, Japan) (CHI '21). Association for Computing Machinery, New York, NY, USA, Article 225, 11 pages. <https://doi.org/10.1145/3411764.3445545>
- [102] Mingdi Xu, Takeshi Tachibana, Nana Suzuki, Eiichi Hoshino, Yuri Terasawa, Norihisa Miki, and Yasuyo Minagawa. 2021. The effect of haptic stimulation simulating heartbeats on the regulation of physiological responses and prosocial behavior under stress: The influence of interoceptive accuracy. *Biological Psychology* 164 (2021), 108172. <https://doi.org/10.1016/j.biopsych.2021.108172>
- [103] Giorgia Zamariola, Elke Vlemmix, Olivier Corneille, and Olivier Luminet. 2018. Relationship between interoceptive accuracy, interoceptive sensibility, and alexithymia. *Personality and Individual Differences* 125 (2018), 14–20. <https://doi.org/10.1016/j.paid.2017.12.024>
- [104] Thorsten O. Zander, Christian Kothe, Sabine Jatzhev, and Matti Gaertner. 2010. *Enhancing Human-Computer Interaction with Input from Active and Passive Brain-Computer Interfaces*. Springer London, London, 181–199. https://doi.org/10.1007/978-1-84996-272-8_11
- [105] Yizhen Zhou, Aiko Murata, and Junji Watanabe. 2020. The Calming Effect of Heartbeat Vibration. In *2020 IEEE Haptics Symposium (HAPTICS)*. 677–683. <https://doi.org/10.1109/HAPTICS45997.2020.ras.HAP20.157.5a2e1551>

A Heartbeat Resonance in New Environments

This code can be used to set up *Heartbeat Resonance* in a new environment. We used Wolfram Kernel 13.3 within a Jupyter Notebook to execute the code. The output of the code is the pressure distribution matrices for all the room modes. These matrices can be used to locate regions of high pressure in the environment.

```

1 (* The speed of sound, in meters per second *)
2 c = QuantityMagnitude[StandardAtmosphereData[Quantity[0, "Meter"], "SoundSpeed"]];
3 (* Define the shape of the room using a basic solid primitive, in this case a cuboid. *)
4 roomDimensions = {1.7, 2.18, 2.12}; (* These values are for the room used in the paper (in meters) *)
5 roomGeometry = Cuboid[{0, 0, 0}, roomDimensions];
6 (* This variable is useful when combining more than one geometries. Here we leave it as such *)
7 model = roomGeometry;
8 (* Visualize the defined cuboid representing the room *)
9 Graphics3D[{Opacity[0.1], {Blue, model}}, ImageSize -> Medium, Axes -> True, AxesLabel -> {x, y, z}, ViewVector -> {15, -15, 15}]
10 (* Convert the model/geometry into a mesh for computation of modes. *)
11 mesh = DiscretizeRegion[model, MeshQualityGoal -> "Maximal", AccuracyGoal -> 4, MaxCellMeasure -> {"Volume" -> 0.001}, PerformanceGoal -> "Quality"];
12 (* Display the solid cuboid model and the generated mesh side by side for visualization *)
13 Grid[{{Graphics3D[{Opacity[0.1], model}, ImageSize -> Medium, ViewVector -> {15, -15, 15}], Graphics3D[{Opacity[0.25], mesh}, ImageSize -> Medium, ViewVector -> {15, -15, 15}]}}]
14 (* Compute the first 'nmodes' acoustic modes of the room. The first mode is at f=0, so we ignore that. *)
15 nmodes = 15;
16 (* The Helmholtz equation (Laplacian) is being solved here. By default, Neumann boundary conditions are assumed in NDEigensystem, meaning the walls are perfectly reflective. This is suitable since we used MDF walls, which are dense and highly reflective. *)
17 AbsoluteTiming[{lambda, eigfun} = NDEigensystem[{-Laplacian[u[x, y, z], {x, y, z}], u[x, y, z], Element[{x, y, z}, mesh], nmodes]];
18 (* Convert the computed eigenvalues into frequencies (Hz). *)
19 freqs = c * Sqrt[lambda] / (2 * Pi);
20 (* Display the frequencies in a grid layout *)
21 Grid[Transpose[{Range[nmodes], freqs}], Alignment -> Right]
22 (* Visualize the acoustic modes within the room. *)
23 plots = Table[DensityPlot3D[eigfun[[mode]], Element[{x, y, z}, model], ColorFunction -> ColorData["RedGreenSplit"], ViewVector -> {15, -15, 15}], {mode, nmodes}]
24 (* Define the grid of points where the pressure field will be evaluated for each mode. *)
25 xValues = Range[0, roomDimensions[[1]], 0.05]; (* x-axis grid points *)
26 yValues = Range[0, roomDimensions[[2]], 0.05]; (* y-axis grid points *)
27 zValues = Range[0, roomDimensions[[3]], 0.05]; (* z-axis grid points *)
28 (* The 'pressureField' variable contains the computed pressure values for all modes. *)
29 pressureField = Table[Table[eigfun[[mode]] /. {x -> xVal, y -> yVal, z -> zVal}, {xVal, xValues}, {yVal, yValues}, {zVal, zValues}], {mode, nmodes}];
30 (* Export the computed pressure field for each mode to .mat files. *)
31 Do[Export["pressure_field_mode_" <> ToString[mode] <> ".mat", pressureField[[mode]], "MAT"], {mode, nmodes}];

```

A.1 Modeling Partial Reflectivity from Walls

The following code adds the reflectivity coefficient for the walls of the environment. Choose a reflectivity value and replace line 17 in the main code with the code below.

```

1 (*To model partial reflectivity, we can introduce impedance boundary conditions. Below is an example of how to modify the boundary conditions to
   include partial absorption. *)
2 reflectivityCoefficient = 0.5; (* Modify this value to change the reflectivity level *)
3 AbsoluteTiming[{lambda, eigfun} = NDEigensystem[{-Laplacian[u[x, y, z], {x, y, z}] + reflectivityCoefficient * u[x, y, z], u[x, y, z], Element
   [{x, y, z}, mesh], nmodes}];

```

A.2 Modeling Objects Inside the Environment

The following code can be used to add objects such as furniture or partitions to the environment. Represent these objects using geometric primitives and replace lines 5–7 in the main code with the code provided below.

```

1 (* Example: Adding furniture inside the room *)
2 (* Other possible primitives: Sphere, Cylinder, Cone, Pyramid, Prism, Polyhedron *)
3 wardrobe = Cuboid[{0.5, 0.5, 0}, {1.0, 1.0, 1.8}]; (* A wardrobe with dimensions 0.5 m x 0.5 m x 1.8 m *)
4 desk = Cuboid[{1.2, 1.0, 0}, {1.6, 1.8, 0.8}]; (* A desk with dimensions 0.4 m x 0.8 m x 0.8 m *)
5 (* Combine the room with the furniture *)
6 model = RegionUnion[roomGeometry, wardrobe, desk];

```

B Detailed Statistics for Experiment 1 (Inducing Heartbeat Sensations)

B.1 Mean Realism and Intensity Data

Conditions		Realism		Intensity	
		Mean	SD	Mean	SD
Basic Heartbeat	78Hz	3.14	0.33	3.18	0.29
	100Hz	2.61	0.24	2.43	0.2
	156Hz	2.64	0.19	2.89	0.2
	200Hz	2.54	0.29	3.43	0.27
Enhanced Heartbeat	78Hz	3.18	0.2	3.29	0.2
	100Hz	2.57	0.28	2.57	0.24
	156Hz	2.5	0.19	2.96	0.25
	200Hz	2.18	0.23	3.29	0.26
Real		2.64	0.4	2.14	0.27

Table 1: This table provides data for Fig. 4a and 4b. Mean and standard deviation (SD) for realism and intensity across different heartbeat conditions. The highest values for realism and intensity are highlighted in bold.

B.2 Realism and Intensity for Modulation Frequencies

Condition		Realism		P-Value		Intensity		P-Value	
		Mean	SD	(Compared to real signal))		Mean	SD	(Compared to real signal)	
Frequencies	78Hz	3.16	0.27	0.03		3.23	0.26	0.0001	
	100Hz	2.59	0.2	0.78		2.5	0.18	0.07	
	156Hz	2.57	0.2	0.87		2.93	0.19	0.002	
	200Hz	2.36	0.16	0.33		3.36	0.17	0.0001	
Real		2.64	0.4			2.14	0.27		

Table 2: This table provides data for Fig. 5a and 5b. Mean and standard deviation (SD) for realism and intensity across different frequencies. The data for basic and enhanced heartbeat signals is combined. The highest values for realism and intensity are highlighted in bold. The significant p-values are also shown in bold, highlighting the frequencies that had a significant effect compared to the real signal.

C Detailed Statistics for Experiment 2 (Perceived Heart Rate Entrainment)

C.1 Confidence-Perception Data

Conditions		Correct		Incorrect		Total Counts
		High Confidence	Low Confidence	High Confidence	Low Confidence	
Heartbeat Resonance	-30	29.4	17.6	35.3	17.6	17
	-15	18.8	31.3	18.8	31.3	16
	15%	50.0	18.8	18.8	12.5	16
	30%	33.3	0.0	16.7	50.0	12
Vibrotactile	-30	23.1	15.4	38.5	23.1	13
	-15	27.3	0.0	45.5	27.3	11
	15%	16.7	25.0	25.0	33.3	12
	30%	13.3	20.0	6.7	60.0	15

Table 3: Percentage distribution of participants' responses by condition, confidence level, and accuracy. The table includes both correct and incorrect responses, categorized by high and low confidence for each condition and modulation level. Data is presented as percentages since Total Counts for high and low confidence differ due to the exclusion of neutral confidence ratings (rating of 3).

C.2 Confidence-Perception Excluding “no change” in Perception

Conditions		Correct % (excluding “no change”)		Incorrect % (excluding “no change”)		Total Counts
		High Confidence	Low Confidence	High Confidence	Low Confidence	
Heratbeat Resonance	-30	38.5	23.1	30.8	7.7	13
	-15	25.0	41.7	8.3	25.0	12
	15%	66.7	25.0	0.0	8.3	12
	30%	57.1	0.0	28.6	14.3	7
Vibrotactile	-30	33.3	22.2	33.3	11.1	9
	-15	33.3	0.0	55.6	11.1	9
	15%	33.3	50.0	0.0	16.7	6
	30%	28.6	42.9	0.0	28.6	7

Table 4: Detailed values for Fig. 11. Percentage distribution of participants’ responses by condition, confidence level, and accuracy, excluding both ‘no change’ responses for perceived heart rate changes and neutral confidence ratings (rating of 3). The table shows correct and incorrect responses categorized by high and low confidence for each condition. Data is presented as percentages since total counts for high and low confidence differ due to the exclusion of neutral confidence ratings. The Total Counts column shows the number of eligible responses for each condition.

C.3 Heart Rate Deviation

Conditions		Median	Q1	Q3	Min	Max	P-Value (in comparison with baseline)
Baseline Resting		0	0	0	0	0	
Heartbeat Resonance	-30%	0.07	-1.52	4.3	-6.34	12.32	0.26
	-15%	-0.63	-4.98	2.55	-12.94	7.49	0.19
	+15%	2.55	-1.86	5.95	-8.03	12.62	0.03
	+30%	0.29	-2.15	5	-5.06	14.2	0.15
Vibrotactile	-30%	0.7	-4	6.37	-11.59	14.02	0.86
	-15%	-0.89	-7.03	5.26	-11.13	18.03	0.29
	+15%	1.39	0.11	5.39	-4.14	7.67	0.08
	+30%	-0.27	-5.23	4	-10.59	8.98	0.96

Table 5: Summary of boxplot statistics from Fig. 12a representing heart rate deviation from baseline across different feedback vonditions. The +15% condition for Heartbeat Resonance was the only one significantly different from the baseline.

C.4 RMSSD

Conditions		Median	Q1	Q3	Min	Max	P-Value (in comparison with baseline)
Baseline Resting		22.02	12.07	35.52	4.02	48.1	
Heartbeat Resonance	-30%	12.44	7.86	19.7	5.04	31.58	0.09
	-15%	13.9	8.02	24.39	5.87	36.18	0.66
	+15%	15.66	8.61	22.76	7.26	30.79	0.93
	+30%	19.17	9.09	28.49	4.24	44.77	0.89
Vibrotactile	-30%	13.33	8.55	24.41	5.05	28.52	0.43
	-15%	13.91	10.09	26.06	7.11	33.38	0.79
	+15%	15.99	10.36	23.55	4.88	38.63	0.29
	+30%	13.62	10.16	24.59	5.75	38.67	0.056

Table 6: Details of boxplots in Fig. 12b. The tables show RMSSD statistics (Median, Q1, Q3, Min, Max) and P-Values for Heart Rate Variability across different conditions compared to baseline resting. The p-values indicate no significant difference between the conditions and the baseline resting state.